Stage de recherche, MIP 2ème année
du 10 janvier au 10 juillet 2002

Thierry Mora
sous la direction de Clifford M. Will

Inspiralling binary systems of compact objects: Comparisons between analytical and numerical results

Systèmes binaires d'objets compacts en phase spirale : comparaisons entre des résultats analytiques et numériques

Washington University Gravity Group (WUGRAV)
McDonnell Center for the Space Sciences
Department of Physics
Washington University in Saint Louis
Saint Louis, Missouri 63130

Contents

Acknowledgments

I first want to thank Clifford M. Will, not only for welcoming me in his group, but also for sustaining a climate of work and stimulation in brand new air-conditioned offices, and for giving me useful advise and directions when my inspiration was dying out.

I am also grateful to Luc Blanchet for willingly producing customized formulae with his all-mighty Mathematica programs, and for giving me opportunities to practice my french.

I finally want to thank Mark Miller and Wai-Mo Suen for fruitful discussion and for providing us with all the data and information we needed for our comparisons.

1 Introduction

Inspiraling binary systems containing very compact objects, like black holes or neutron stars, are considered to be among the most promising sources of gravitational waves for laser interferometric detectors such as LIGO (Caltech-MIT) or VIRGO (France-Italy). Because of gravitational-radiation reaction (relativistic equivalent to electromagnetic Larmor effect), the orbit of compact binaries is expected to shrink progressively before the bodies eventually merge together. Naturally, the amplitude of the gravitational-wave emissions will increase as the separation between the two bodies decreases (and as their velocity increases). For that reason the late stage of inspiral prior to coalescence, for which the gravitational emissions are supposed to be the strongest, has become a focus of high interest in the past few years. The main challenge lies in the characterization of the gravitational waves we expect to detect, and in the search for methods allowing to extract information from the waveform, such as the masses involved in the system, or the nature of the body resulting from the merger (probably a black hole). In order to meet this challenge, one needs to characterize the motion of the binary on the one hand, and the gravitational flux generated by this motion on the other hand. Both phenomena are coupled, since the motion is affected by the gravitational field it generates by back-reaction.

Two different approaches have been proposed to handle the problem:

- The post-Newtonian treatment, relying on the expansion of solutions of Einstein's equations in powers of v^2/c^2 (v being the typical velocity of the system) applied to the two-body problem.

- The numerical treatment, which consists in solving the full Einstein equations on computers.

1.1 Post-Newtonian methods

Post-Newtonian techniques have proved particularly accurate for describing the early stage of inspiral. One can show, either from the post-Newtonian equations of motion or from the gravitationial waveform, that the relative motion tends to evolve towards a circular orbit when submitted to gravitational-radiation reaction. By the time the gravitational flux is strong enough to be detectable by laser interferometric antennas (10^{-22} relative perturbation to the background metric out to 100 Mpc), the orbit will have become "quasi-circular". It will actually be slightly spiral (hence the prefix "quasi") because of the decay, but we will assume the evolution to be adiabatic, and we will consider that the orbit evolves smoothly from one circular orbit to the other.

Recent estimates suggest that reasonably common events will generate a very weak signal to noise ratio in current detectors. Methods of *matched filtering*, which consist in using known templates to extract the signal from the noise, have been developped to overcome this difficulty. However, one has to predict the *phase* of the signal with very high accuracy to implement this method.

In order to compute the phase we can use the energy balance equation:

$$\frac{\mathrm{d}E}{\mathrm{d}t} = -\mathcal{L}, \tag{1}$$

where E is the total center-of-mass energy of the binary, and $\mathcal{L}$ the gravitational "luminosity" of the source—*i.e.* the gravitational energy flux as seen from infinity—and express these two quantities in terms of the characteristics of the motion. At leading order, the center-of-mass energy reads:

$$E = -\frac{G\mu m}{2a}, \tag{2}$$

where a is the semimajor axis, μ the reduced mass and m the total mass. The total luminosity is given at leading order by the Einstein quadrupole formula:

$$\mathcal{L} = \frac{G}{5c^5}\frac{\mathrm{d}^3Q_{ab}}{\mathrm{d}t^3}\frac{\mathrm{d}^3Q_{ab}}{\mathrm{d}t^3} = \frac{8G^3}{5c^5}\eta^2\left(\frac{m}{r}\right)^4\left(12v^2 - 11\dot{r}^2\right), \tag{3}$$

where Q_{ab} is the trace-free quadrupole moment tensor of the source, r the separation between the two bodies, v the relative velocity, $\eta = \mu/m$, and where we use the Einstein summation convention.

This quadrupole formula, directly derived from the equations of general relativity, has been proved to agree with the observation of the dynamics of the binary pulsar 1913+16 [1]. Indeed, using (1), (2) and (3), one can characterize the decay of the orbit by:

$$\dot{T} = -\frac{192\pi G^{5/3}\eta m^{-2/3}}{5c^5}\left(\frac{T}{2\pi}\right)^{-5/3}\left(1-e^2\right)^{-7/2}\left(1+\frac{73}{24}e^2+\frac{73}{96}e^4\right), \tag{4}$$

where T is the orbital period. This formula perfectly agrees with the observations, which gives an indirect evidence of the existence of gravitational waves and a strong support to general relativity.

Nevertheless, direct detection of gravitational waves necessitates very accurate expressions of the phase. For that purpose post-Newtonian (PN) extensions of (2) and (3) have been computed through 3.5 PN order ($O(v/c)^7$) beyond the leading order). The expression of the energy largely depends on the expression of the equations of motion, which have been computed by several groups [12]-[24] (see section 2.5 for more details). As for the waveform, and hence the luminosity, they have been computed by two different groups through the second post-Newtonian order in 1995 [2, 3, 4], and more recently up to 3.5 order by Blanchet *et al.* [5].

We can now make use of the fact that the orbit is quasi-circular. In that particular case, we have formulae of the type [6]:

$$E = -\frac{\mu c^2 x}{2}\left(1+\lambda_1 x+\lambda_2 x^2+\cdots\right), \tag{5}$$

$$\mathcal{L} = \frac{32\eta^2 c^5}{5G}x^5\left(1+\mu_1 x+\mu_2 x^2+\cdots\right), \tag{6}$$

$$\text{with} \quad x = \frac{(Gm\omega)^{2/3}}{c^2}, \tag{7}$$

where ω is the angular velocity of the relative motion. Combining these two equations with (1), one can find a 3.5 post-Newtonian accurate expression of the phase (see [6] for a complete computation). It was actually shown that a 3PN order accuracy was required to use effectively the filtering techniques mentioned before.

We claimed that the post-Newtonian equations were effective for the early stage of inspiral, *i.e.* for large separations. For short separations however, where high velocities and strong gravitational fields are implied, the post-Newtonian approximation is no longer valid. Moreover, finite-size effects (formally of the fifth post-Newtonian order) will have to be taken into account in the case of neutron stars, where they have a considerable influence.

1.2 Numerical solutions

At regimes where the confidence in post-Newtonian formulae ends, the problem has to be handled numerically. Numerical simlulations are usually implemented within the framework of the so-called "3+1" formulation of general relativity, which relies on the separation between space and time in Einstein's equations. The first stage is to solve the initial value problem consisting of two constraint equations (the Hamiltonian and the momentum constraints) which account for four of the ten Einstein equations. Then, starting off with this initial value data set, one can evolve the system using the six remaining Einstein equations.

A couple of additionnal assumptions are made to make the initial value problem more tractable numerically. First it is imposed that the initial state is a perfect circular orbit, consistently with the post-Newtonian prediction. This is supposedly satisfied by the existence of an initial "helical Killing vector" of the type $\frac{\partial}{\partial t} + \Omega \frac{\partial}{\partial \phi}$, which ensures that the state of the system is invariant along this space-time direction. This condition actually corresponds to a *local* condition of circularity whose basic translation into post-Newtonian language is $\dot{r} = 0$, and accounts for one additionnal Einstein equation. Besides, this assumption amounts to ignoring radiation reaction in the initial state, which should give birth to anti-damping effects in the evolution. Secondly, convenient but arbitrary assumptions are made, such as the conformal flatness of the spatial metric, that may introduce errors in the generated solutions. This latter approximation is usually justified by the neglect of radiation reaction in the initial data.

Along with the relativistic equations, one has to impose horizon boundary conditions for black hole binaries, and to provide a realistic (usually polytropic) equation of state for neutron star binaries.

In order to fully understand the inspiral of compact binaries, one would like to know how to connect the post-Newtonian regime to the numerical regime. This is not as easy as one might think because numerical simulations, which are limited by computational resources, cannot always be started with large separations where the post-Newtonian approximation is believed to be valid. For neutron stars however, separations are perforce larger because of the size of the bodies themselves, but in that case finite-size effects cannot be neglected.

Two important covariant quantities generated by both post-Newtonian and numerical approaches are the total energy and secondarily the total angular momentum of the system. They can both be expressed as functions of the orbital frequency Ω, which is a covariant quantity in the case of circular orbits, and are therefore good candidates for making comparisons between post-Newtonian and numerical results.

We have developed post-Newtonian formulae for $E(\Omega)$ and $J(\Omega)$ at the apastron or periastron (where $\dot{r} = 0$) for arbitrary eccentric orbits in three different cases corresponding to three different initial-data numerical simulations:

- Corotational black hole simulation [7]. Since the stars are corotating (spinning with the same angular velocity as the orbital frequency), we will have to add spin contributions. The black holes will be considered to be point-masses.
- Irrotational neutron star simulation [8]. In that case we will have to include Newtonian tidal interaction terms.
- Corotational neutron star simulation (Mark Miller *et al.*). This simulation has been adapted for our purpose: we have been provided with the total energy of the binary from which the energy of each star taken in an isolated state and spinning with the same angular velocity has been substracted off, so that the resulting energy is purely orbital. In that case we will have to add spin-orbit and tidal contributions.

It has been estimated that by the time a compact binary reaches coalescence it will not have been synchronized by tidal viscosity. This means that the corotational assumption is not expected to be fulfilled, even though it makes the numerical problem easier to handle (in that case the velocity field for the matter is proportional to the helical Killing vector).

The remainder of this report gives the details of the computations leading to the comparison between post-Newtonian formulae and numerical data. First, we will describe the methods used to solve the post-Newtonian equations of motion, and check their consistency with previous results. Then a hydrodynamic model will be presented, and applied to the case of two identical neutron stars. Finally, we will attempt to fit the numerical data with our theoretical curves. The results will be discussed for each case.

2 Solution to the post-Newtonian equations of motion

2.1 Equations of motion

The two-body problem has been solved for long in the Newtonian case. However, for very massive bodies, as the Newtonian approximation becomes inappropriate, new equations including corrections due to general relativity are required. These corrections are expressed as an expansion in powers of $\epsilon \approx v^2/c^2 \approx Gm/rc^2$. The leading term of this expansion will be the Newtonian term. Then will follow the so-called post-Newtonian (PN) contributions.

We use the standard form of the equations of motion, written in a "Newtonian-like" manner:

$$\begin{aligned} \mathbf{a}_1 &= \frac{\mathrm{d}^2\mathbf{x}_1}{\mathrm{d}t^2} = \frac{m_2}{r^2}\Big\{\mathbf{n}[-1 + (PN) + (P^2N) + (P^{5/2}N) + (P^3N) + (P^{7/2}N) + \cdots] \\ &\quad +\mathbf{v}[(PN) + (P^2N) + (P^{5/2}N) + (P^3N) + (P^{7/2}N) + \cdots]\Big\}, \end{aligned} \tag{8}$$

where $\mathbf{x}_a$ and m_a denote the position and the mass of the body a, $\mathbf{n}$ is the unit vector from 1 to 2, $\mathbf{v}$ the relative velocity, and r the separation between the two bodies. Henceforth we use units in which $G = c = 1$. The notation P^nN represents the n^{th} post-Newtonian correction to Newtonian gravity. These equations are valid only for point-like, non-spinning bodies. As such, according to the "effacement" principle, which is a extention of the strong equivalence principle, they should not depend on the internal structure of the bodies, but only on their masses. This expansion has two limitations: (i) for short separations (and big velocities), the approximation $\epsilon \ll 1$ is expected to break down. In that case the PN expansion—which is known to a finite order—is no longer valid; (ii) in real systems, the bodies will not be exact point-masses, and finite-size effects will have to be included.

Post-Newtonian terms P^nN include even ($2n$ even) and odd ($2n$ odd) orders. Even terms are conservative, in the sense that we can associate a conserved energy to them. Odd terms correspond to the radiation reaction energy loss, and therefore are not conservative. In particular, as we shall see in detail, they will cause the orbit to shrink, and the eccentricity to decrease.

For more convenience, we convert the two-body problem to an effective one-body problem. For this purpose we choose the origin to be at the center of mass of the system, which is defined by an integral of the motion. Then we change the variables to the relative coordinates $\mathbf{x} = \mathbf{x}_1 - \mathbf{x}_1$ and, using relations of the type:

$$\begin{aligned} \mathbf{x}_1 &= [m_2/m + (PN) + \cdots]\mathbf{x}, \\ \mathbf{x}_2 &= [-m_1/m + (PN) + \cdots]\mathbf{x}, \end{aligned} \tag{9}$$

where $m = m_1 + m_2$ is the total mass of the system, we obtain the equations of motion in terms of relative coordinates:

$$\mathbf{a} = \frac{\mathrm{d}^2\mathbf{x}}{\mathrm{d}t^2} = \frac{m}{r^2}\left[(-1 + A)\mathbf{n} + B\mathbf{v}\right], \tag{10}$$

where A and B include post-Newtonian terms. So far, equations of motion have been computed up to 3.5^{th} order. In an appropriate harmonic gauge, writing $A = A_1 + A_2 + \cdots$

and $B = B_1 + B_2 + \cdots$, the expressions for A and B read:

$$A_1 = 2(2+\eta)\frac{m}{r} - (1+3\eta)v^2 + \frac{3}{2}\eta\dot{r}^2, \tag{11}$$

$$\begin{aligned} A_2 = & -\frac{3}{4}(12+29\eta)\left(\frac{m}{r}\right)^2 - \eta(3-4\eta)v^4 - \frac{15}{8}\eta(1-3\eta)\dot{r}^4 \\ & + \frac{3}{2}\eta(3-4\eta)v^2\dot{r}^2 + \frac{1}{2}\eta(13-4\eta)\frac{m}{r}v^2 + (2+25\eta+2\eta^2)\frac{m}{r}\dot{r}^2, \end{aligned} \tag{12}$$

$$A_{5/2} = \frac{8}{5}\eta\frac{m}{r}\dot{r}\left(3v^2 + \frac{17}{3}\frac{m}{r}\right), \tag{13}$$

$$\begin{aligned} A_3 = & \left[16 + \left(\frac{14997}{140} - \frac{41}{16}\pi^2 - \frac{44}{3}\lambda\right)\eta + \frac{71}{2}\eta^2\right]\left(\frac{m}{r}\right)^3 - \frac{1}{4}\eta(11-49\eta+52\eta^2)v^6 \\ & + \frac{35}{16}\eta(1-7\eta+7\eta^2)\dot{r}^6 + \eta\left(\frac{20827}{840} + \frac{123}{64}\pi^2 - \eta^2\right)\left(\frac{m}{r}\right)^2 v^2 \\ & - \left[1 + \left(\frac{22717}{168} + \frac{615}{64}\pi^2\right)\eta + \frac{11}{8}\eta^2 - 7\eta^3\right]\left(\frac{m}{r}\right)^2\dot{r}^2 \\ & - \eta\left(\frac{75}{4} + 8\eta - 10\eta^2\right)\frac{m}{r}v^4 + \eta\left(\frac{15}{2} - \frac{237}{8}\eta + \frac{45}{2}\eta^2\right)v^4\dot{r}^2 \\ & - \eta\left(79 - \frac{69}{2}\eta - 30\eta^2\right)\frac{m}{r}\dot{r}^4 - \frac{15}{8}\eta\left(4 - 18\eta + 17\eta^2\right)v^2\dot{r}^4 \\ & + \eta\left(121 - 16\eta - 20\eta^2\right)\frac{m}{r}v^2\dot{r}^2, \end{aligned} \tag{14}$$

$$\begin{aligned} A_{7/2} = & -\frac{8}{5}\eta\frac{m}{r}\dot{r}\left[\frac{3}{28}(61+70\eta)v^4 + \frac{1}{42}(519-1267\eta)\frac{m}{r}v^2 - \frac{15}{4}(19+2\eta)v^2\dot{r}^2 \right. \\ & \left. + \frac{1}{4}(147+188\eta)\frac{m}{r}\dot{r}^2 + 70\dot{r}^3 + \frac{23}{14}(43+14\eta)\left(\frac{m}{r}\right)^2\right], \end{aligned} \tag{15}$$

$$B_1 = 2(2-\eta)\dot{r} \tag{16}$$

$$B_2 = \frac{1}{2}\dot{r}\left[\eta(15-4\eta)v^2 - (4+41\eta+8\eta^2)\frac{m}{r} - 3\eta(3+2\eta)\dot{r}^2\right], \tag{17}$$

$$B_{5/2} = -\frac{8}{5}\eta\frac{m}{r}\left(v^2 + 3\frac{m}{r}\right), \tag{18}$$

$$\begin{aligned} B_3 = & \left[4 + \left(\frac{5849}{840} + \frac{123}{32}\pi^2\right)\eta - 25\eta^2 - 8\eta^3\right]\left(\frac{m}{r}\right)^2 + \eta\left(\frac{65}{8} - 19\eta - 6\eta^2\right)v^4 \\ & + \eta\left(\frac{45}{8} - 15\eta - \frac{15}{4}\eta^2\right)\dot{r}^4 + \eta\left(15 + 27\eta + 10\eta^2\right)\frac{m}{r}v^2 \\ & - \eta\left(\frac{329}{6} + \frac{59}{2}\eta + 18\eta^2\right)\frac{m}{r}\dot{r}^2 - \eta\left(12 - \frac{111}{4}\eta - 12\eta^2\right)v^2\dot{r}^2, \end{aligned} \tag{19}$$

$$\begin{aligned} B_{7/2} = & \frac{8}{5}\eta\frac{m}{r}\left[\frac{1}{28}(313+42\eta)v^4 - \frac{1}{42}(205+777\eta)\frac{m}{r}v^2 - \frac{3}{4}(113+2\eta)v^2\dot{r}^2 \right. \\ & \left. + \frac{1}{12}(205+424\eta)\frac{m}{r}\dot{r}^2 + 75\dot{r}^4 + \frac{1}{42}(1325+546\eta)\left(\frac{m}{r}\right)^2\right]. \end{aligned} \tag{20}$$

Using the general relation for circular Keplerian orbits $v^2 = m/r$, we have $m/r \approx \epsilon$. $\dot{r}$ is the radial velocity $\mathbf{v}\cdot\mathbf{n}$, and is of order $\epsilon^{1/2}$. η is the mass ratio $m_1 m_2/m^2$.

We can associate two useful quantities with the conservative part of these orbital equations, namely the total energy E and the total angular momentum $\mathbf{J}$. Writing $E = E_0 + E_1 + E_2 + E_3$ and $\mathbf{J} = \mathbf{J}_0 + \mathbf{J}_1 + \mathbf{J}_2 + \mathbf{J}_3$, we have:

$$E_0/\mu = \frac{1}{2}v^2 - \frac{m}{r} \tag{21}$$

$$E_1/\mu = \frac{3}{8}(1-3\eta)v^4 + \frac{1}{2}(3+\eta)v^2\frac{m}{r} + \frac{1}{2}\eta\frac{m}{r}\dot{r}^2 + \frac{1}{2}\left(\frac{m}{r}\right)^2 \tag{22}$$

$$\begin{aligned} E_2/\mu = {} & \frac{5}{16}(1-7\eta+13\eta^2)v^6 + \frac{1}{8}(21-23\eta-27\eta^2)\frac{m}{r}v^4 + \frac{1}{4}\eta(1-15\eta)\frac{m}{r}v^2\dot{r}^2 \\ & -\frac{3}{8}\eta(1-3\eta)\frac{m}{r}\dot{r}^4 + \frac{1}{8}(14-55\eta+4\eta^2)\left(\frac{m}{r}\right)^2 v^2 \\ & +\frac{1}{8}(4+69\eta+12\eta^2)\left(\frac{m}{r}\right)^2\dot{r}^2 - \frac{1}{4}(2+15\eta)\left(\frac{m}{r}\right)^3, \end{aligned} \tag{23}$$

$$\begin{aligned} E_3/\mu = {} & \left[\frac{3}{8} + \left(\frac{2747}{140} - \frac{11}{3}\lambda\right)\eta\right]\left(\frac{m}{r}\right)^4 + \frac{1}{128}\left(35-413\eta+1666\eta^2-2261\eta^3\right)v^8 \\ & + \left[\frac{5}{4} - \left(\frac{6747}{280} - \frac{41}{64}\pi^2\right)\eta - \frac{21}{4}\eta^2 + \frac{1}{2}\eta^3\right]\left(\frac{m}{r}\right)^3 v^2 \\ & + \left[\frac{3}{2} + \left(\frac{2321}{280} - \frac{123}{64}\pi^2\right)\eta + \frac{51}{4}\eta^2 + \frac{7}{2}\eta^3\right]\left(\frac{m}{r}\right)^3\dot{r}^2 + \\ & \frac{1}{16}(55-215\eta+116\eta^2+325\eta^3)\frac{m}{r}v^6 + \frac{1}{16}\eta(5-25\eta+25\eta^2)\frac{m}{r}\dot{r}^6 \\ & +\frac{1}{16}(135-194\eta+406\eta^2-108\eta^3)\left(\frac{m}{r}\right)^2 v^4 \\ & -\frac{1}{48}\eta(731-492\eta-288\eta^2)\left(\frac{m}{r}\right)^2\dot{r}^4 \\ & +\frac{1}{16}(12+248\eta-815\eta^2-324\eta^3)\left(\frac{m}{r}\right)^2 v^2\dot{r}^2 \\ & -\frac{1}{16}\eta(21+75\eta-375\eta^2)\frac{m}{r}v^4\dot{r}^2 - \frac{1}{16}\eta(9-84\eta+165\eta^2)\frac{m}{r}v^2\dot{r}^4, \end{aligned} \tag{24}$$

$$\mathbf{J}_0 = \mu(\mathbf{r}\times\mathbf{v}) \tag{25}$$

$$\mathbf{J}_1 = \mu(\mathbf{r}\times\mathbf{v})\left[(3+\eta)\frac{m}{r} + \frac{1}{2}(1-3\eta)v^2\right] \tag{26}$$

$$\begin{aligned} \mathbf{J}_2 = {} & \mu(\mathbf{r}\times\mathbf{v})\left[\frac{1}{4}(14-41\eta+4\eta^2)\left(\frac{m}{r}\right)^2 + \frac{3}{8}(1-7\eta+13\eta^2)v^4\right. \\ & \left. +\frac{1}{2}(7-10\eta-9\eta^2)\frac{m}{r}v^2 - \frac{1}{2}\eta(2+5\eta)\frac{m}{r}\dot{r}^2\right], \end{aligned} \tag{27}$$

$$\begin{aligned} \mathbf{J}_3 = {} & \mu(\mathbf{r}\times\mathbf{v})\left\{\left[\frac{5}{2} - \left(\frac{5199}{280} - \frac{41}{32}\pi^2\right)\eta - 7\eta^2 + \eta^3\right]\left(\frac{m}{r}\right)^3\right. \\ & +\frac{1}{16}(5-59\eta+238\eta^2-323\eta^3)v^6 \\ & +\frac{1}{12}(135-322\eta+315\eta^2-108\eta^3)\left(\frac{m}{r}\right)^2 v^2 \end{aligned}$$

$$+\frac{1}{24}(12-287\eta-951\eta^2-324\eta^3)\left(\frac{m}{r}\right)^2\dot{r}^2$$
$$+\frac{1}{8}(33-142\eta+106\eta^2+195\eta^3)\frac{m}{r}v^4+\frac{3}{8}\eta(2-2\eta-11\eta^2)\frac{m}{r}\dot{r}^4\bigg\}, \qquad (28)$$

where μ is the reduced mass m_1m_2/m. These are constants of the motion provided that the radiation damping caused by $P^{5/2}N$ and $P^{7/2}N$ terms is ignored.

2.2 Osculating orbits elements and planetary equations

In order to solve these equations, we shall adopt a formalism involving orbital osculating elements. Such an approach is expected to be fruitful, since we are dealing with a perturbed two-body problem. The osculating elements basically describe the Keplerian orbit that would be tangent to the actual trajectory at a particular moment. In the Newtonian case, the osculating elements are constant; in a perturbed Newtonian problem, they change smoothly with time (see [9] for more details about the method of osculating elements applied to the post-Newtonian problem).

From the equations of motion we can easily deduce that the trajectory is planar, which allows us to reduce the number of variables from six to four. If we assume that the plane of the motion is perpendicular to $\mathbf{z}$ (x, y, z being a standard cartesian coordinate system), our new set of variables (α, β, p, ϕ) is related to the old one (x, y, v_x, v_y) by the definitions:

$$x = r\cos\phi, \qquad (29)$$
$$y = r\sin\phi, \qquad (30)$$
$$v_x = -(m/p)^{1/2}(\beta+\sin\phi), \qquad (31)$$
$$v_y = (m/p)^{1/2}(\alpha+\cos\phi), \qquad (32)$$
$$\text{with} \quad p/r = 1+\alpha\cos\phi+\beta\sin\phi. \qquad (33)$$

Reciprocally, we can deduce the osculating elements from the orbital variables by using the following relations:

$$\phi = 2\arctan\left(\frac{y}{x+r}\right), \qquad (34)$$
$$\alpha = \frac{\sigma}{m}v_y-\cos\phi, \qquad (35)$$
$$\beta = -\frac{\sigma}{m}v_x-\sin\phi, \qquad (36)$$
$$p = r(1+\alpha\cos\phi+\beta\sin\phi), \qquad (37)$$
$$\text{with} \quad \sigma = (\mathbf{r}\times\mathbf{v})\cdot\mathbf{z}. \qquad (38)$$

These additional expressions will also be useful:

$$\dot{r} = (m/p)^{1/2}(\alpha\sin\phi-\beta\cos\phi) \qquad r^2\dot{\phi} = (mp)^{1/2}. \qquad (39)$$

The quantity p is called the semi-latus rectum. We note that the vector (α, β) has the norm of the ordinary Keplerian eccentricity e and the direction ω of the Keplerian periastron, so that we have: $\alpha = e\sin\omega$ and $\beta = e\cos\omega$.

In what follows, we will use the parameter $u = m/p$ rather than p. Note that u is of order ϵ. In the Newtonian case, u, α and β are constants of the motion; in the post-Newtonian problem, these parameters vary according to the following Lincoln-Will planetary equations:

$$\frac{\mathrm{d}u}{\mathrm{d}\phi} = -2u^{3/2}B, \tag{40}$$

$$\frac{\mathrm{d}\alpha}{\mathrm{d}\phi} = A\sin\phi + 2u^{1/2}B(\alpha+\cos\phi), \tag{41}$$

$$\frac{\mathrm{d}\beta}{\mathrm{d}\phi} = -A\cos\phi + 2u^{1/2}B(\beta+\sin\phi), \tag{42}$$

where we have used (29)-(39) and (10).

When the definition of $\mathbf{x}$ and $\mathbf{v}$ [(29)-(32)] are replaced into the expressions of A and B [(11)-(20)], we get coupled first-order differential equations of the variables $\alpha(\phi)$, $\beta(\phi)$ and $u(\phi)$.

2.3 Iterative resolution of the planetary equations

The Lincoln-Will planetary equations derived from (40)-(42) are too long to be reproduced here (they can be found through 2.5PN order in [9]). However we can schematically write them in the general form:

$$\frac{\mathrm{d}u}{\mathrm{d}\phi} = \epsilon\mathcal{D}u_1(\alpha,\beta,u,\tilde{\phi}) + \epsilon^2\mathcal{D}u_2(\alpha,\beta,u,\tilde{\phi}) + \epsilon^{5/2}\mathcal{D}u_{5/2}(\alpha,\beta,u,\tilde{\phi}) + \cdots \tag{43}$$

$$\frac{\mathrm{d}\alpha}{\mathrm{d}\phi} = \epsilon\mathcal{D}\alpha_1(\alpha,\beta,u,\tilde{\phi}) + \epsilon^2\mathcal{D}\alpha_2(\alpha,\beta,u,\tilde{\phi}) + \epsilon^{5/2}\mathcal{D}\alpha_{5/2}(\alpha,\beta,u,\tilde{\phi}) + \cdots \tag{44}$$

$$\frac{\mathrm{d}\beta}{\mathrm{d}\phi} = \epsilon\mathcal{D}\beta_1(\alpha,\beta,u,\tilde{\phi}) + \epsilon^2\mathcal{D}\beta_2(\alpha,\beta,u,\tilde{\phi}) + \epsilon^{5/2}\mathcal{D}\beta_{5/2}(\alpha,\beta,u,\tilde{\phi}) + \cdots \tag{45}$$

$\mathcal{D}u_i$, $\mathcal{D}\alpha_i$ and $\mathcal{D}\beta_i$ ($i \in \{1, 2, 5/2, 3, 7/2\}$) are polynomials of α and β, and simple trigonometric functions of ϕ. When the dependence in ϕ is 2π periodic, we shall use the notation $\tilde{\phi} = \phi\ [2\pi]$ instead of ϕ. The parameter ϵ has been introduced solely to indicate the post-Newtonian order, and it shall be set to 1 in the final results.

We want to solve these equations iteratively. For that purpose we expand the variables in powers of ϵ:

$$\alpha = \tilde{\alpha} + \epsilon\alpha_1(\tilde{\alpha},\tilde{\beta},\tilde{u},\tilde{\phi}) + \epsilon^2\alpha_2(\tilde{\alpha},\tilde{\beta},\tilde{u},\tilde{\phi}) + \cdots, \tag{46}$$

$$\beta = \tilde{\beta} + \epsilon\beta_1(\tilde{\alpha},\tilde{\beta},\tilde{u},\tilde{\phi}) + \epsilon^2\beta_2(\tilde{\alpha},\tilde{\beta},\tilde{u},\tilde{\phi}) + \cdots, \tag{47}$$

$$u = \tilde{u} + \epsilon u_1(\tilde{\alpha},\tilde{\beta},\tilde{u},\tilde{\phi}) + \epsilon^2 u_2(\tilde{\alpha},\tilde{\beta},\tilde{u},\tilde{\phi}) + \cdots. \tag{48}$$

In the iterative procedure, $\tilde{\alpha}$, $\tilde{\beta}$ and $\tilde{u}$ result from the 0 order analysis, and are arbitrary. We we push to higher orders, we will see that these parameters evolve with ϕ. However, we will distinguish between the function $\tilde{\alpha}(\phi)$ and the explicit parameter $\tilde{\alpha}$ involved in α_i, β_i and u_i. Then the total derivative with respect to ϕ reads:

$$\frac{\mathrm{d}}{\mathrm{d}\phi} = \frac{\partial}{\partial\tilde{\phi}} + \frac{\mathrm{d}\tilde{\alpha}}{\mathrm{d}\phi}\frac{\partial}{\partial\tilde{\alpha}} + \frac{\mathrm{d}\tilde{\beta}}{\mathrm{d}\phi}\frac{\partial}{\partial\tilde{\beta}} + \frac{\mathrm{d}\tilde{u}}{\mathrm{d}\phi}\frac{\partial}{\partial\tilde{u}}. \tag{49}$$

We also expand $\mathrm{d}\tilde{\alpha}/\,\mathrm{d}\phi$ in powers of ϵ:

$$\frac{\mathrm{d}\tilde{\alpha}}{\mathrm{d}\phi} = \epsilon d\tilde{\alpha}_1(\tilde{\alpha}_0, \tilde{\beta}_0, \tilde{u}_0) + \epsilon^2 d\tilde{\alpha}_2(\tilde{\alpha}_0, \tilde{\beta}_0, \tilde{u}_0) + \cdots \quad (50)$$

$$\frac{\mathrm{d}\tilde{\beta}}{\mathrm{d}\phi} = \epsilon d\tilde{\beta}_1(\tilde{\alpha}_0, \tilde{\beta}_0, \tilde{u}_0) + \epsilon^2 d\tilde{\beta}_2(\tilde{\alpha}_0, \tilde{\beta}_0, \tilde{u}_0) + \cdots \quad (51)$$

$$\frac{\mathrm{d}\tilde{u}}{\mathrm{d}\phi} = \epsilon d\tilde{u}_1(\tilde{\alpha}_0, \tilde{\beta}_0, \tilde{u}_0) + \epsilon^2 d\tilde{u}_2(\tilde{\alpha}_0, \tilde{\beta}_0, \tilde{u}_0) + \cdots \quad (52)$$

Now we have reduced our study to the search for α_i, β_i, u_i on the one hand, and $d\tilde{\alpha}_i$, $d\tilde{\beta}_i$, $d\tilde{u}_i$ on the other hand. Note that this way of decomposing the problem is somehow arbitrary. However, it turns out to be the most natural one as we solve the equations.

We define the average and the average-free part of a function $f(\tilde{\phi})$ by:

$$\langle f\rangle = \frac{1}{2\pi}\int_0^{2\pi} f(\tilde{\phi})\,\mathrm{d}\tilde{\phi}, \quad (53)$$

$$\mathcal{AF}(f)(\tilde{\phi}) = f(\tilde{\phi}) - \langle f\rangle. \quad (54)$$

We now rewrite (40)-(42) with our new variables, and we collect terms of common powers of ϵ. At first order we get for α:

$$d\tilde{\alpha}_1 + \frac{\partial\alpha_1}{\partial\tilde{\phi}} = \mathcal{D}\alpha_1(\tilde{\alpha}, \tilde{\beta}, \tilde{u}, \tilde{\phi}). \quad (55)$$

Since $\tilde{\alpha}$ does not depend on $\tilde{\phi}$, we deduce:

$$d\tilde{\alpha}_1 = \langle\mathcal{D}\alpha_1\rangle, \quad (56)$$

$$\alpha_1 = \mathcal{AF}\left(\int \mathcal{AF}(\mathcal{D}\alpha_1)(\tilde{\phi})\,\mathrm{d}\tilde{\phi}\right). \quad (57)$$

The role of the second $\mathcal{AF}$ is to get rid of the constant of integration. The same method yields similar results for β and u. Then we get, at second order:

$$\begin{aligned} d\tilde{\alpha}_2 + \frac{\partial\alpha_2}{\partial\tilde{\phi}} &= \mathcal{D}\alpha_2 + \frac{\partial\mathcal{D}\alpha_1}{\partial\alpha}\alpha_1 + \frac{\partial\mathcal{D}\alpha_1}{\partial\beta}\beta_1 + \frac{\partial\mathcal{D}\alpha_1}{\partial u}u_1 - \frac{\partial\alpha_1}{\partial\tilde{\alpha}}d\tilde{\alpha}_1 - \frac{\partial\alpha_1}{\partial\tilde{\beta}}d\tilde{\beta}_1 - \frac{\partial\alpha_1}{\partial\tilde{u}}d\tilde{u}_1 \\ &\equiv f_2(\tilde{\alpha}, \tilde{\beta}, \tilde{u}, \tilde{\phi}), \end{aligned} \quad (58)$$

where α_1, β_1, u_1, $d\tilde{\alpha}_1$, $d\tilde{\beta}_1$ and $d\tilde{u}_1$ are known from the resolution at first order. For the same reasons as previously we have:

$$d\tilde{\alpha}_2 = \langle f_2\rangle, \quad (59)$$

$$\alpha_2 = \mathcal{AF}\left(\int \mathcal{AF}(f_2)(\tilde{\phi})\,\mathrm{d}\tilde{\phi}\right). \quad (60)$$

Using this procedure systematically up to 3.5$^{\text{th}}$ order, we completely determine $\alpha(\tilde{\alpha}, \tilde{\beta}, \tilde{u}, \tilde{\phi})$, $\beta(\tilde{\alpha}, \tilde{\beta}, \tilde{u}, \tilde{\phi})$ and $u(\tilde{\alpha}, \tilde{\beta}, \tilde{u}, \tilde{\phi})$, as well as $\frac{\mathrm{d}\tilde{\alpha}}{\mathrm{d}\phi}(\tilde{\alpha}, \tilde{\beta}, \tilde{u})$, $\frac{\mathrm{d}\tilde{\beta}}{\mathrm{d}\phi}(\tilde{\alpha}, \tilde{\beta}, \tilde{u})$ and $\frac{\mathrm{d}\tilde{u}}{\mathrm{d}\phi}(\tilde{\alpha}, \tilde{\beta}, \tilde{u})$. From this and (29)-(33) we can deduce the expressions of $\mathbf{x}$, $\mathbf{v}$, r, *etc.*

In order to discuss the results, we define $\tilde{e}$ and $\tilde{\omega}$ by $\tilde{\alpha} + i\tilde{\beta} = \tilde{e}\exp(i\tilde{\omega})$. $\tilde{e}$ can be viewed as a post-Newtonian eccentricity and $\tilde{\omega}$ as a post-Newtonian periastron angle. We note that $\tilde{u}$ and $\tilde{e}$ are constant in a conservative motion, *i.e.* when 2.5PN and 3.5PN orders are ignored. Their evolution is given by the coupled equations:

$$\begin{aligned}\frac{\mathrm{d}\tilde{u}}{\mathrm{d}\phi} &= \frac{8}{5}\eta\left(8+7\tilde{e}^2\right)\tilde{u}^{7/2} \\ &\quad -\frac{1}{210}\left[22071+2016\eta-(6064+7112\eta)\tilde{e}^2-(1483+4424\eta)\tilde{e}^4\right]\tilde{u}^{9/2} \qquad (61)\\ \frac{\mathrm{d}\tilde{e}}{\mathrm{d}\phi} &= -\frac{1}{15}\eta\tilde{e}\left(304+121\tilde{e}^2\right)\tilde{u}^{5/2}+\frac{1}{840}\eta\tilde{e}\left[144392+45696\eta\right.\\ &\quad \left.-(34768+10892\eta)\tilde{e}^2-(2251-5096\eta)\tilde{e}^4\right]\tilde{u}^{7/2} \qquad (62)\end{aligned}$$

We note that the eccentricity decreases as the orbit shrinks, so that the orbit gets closer and closer to a perfect spiral. Along with this, we observe a phenomenon of periastron advance, which is driven by the conservative part of the equations:

$$\begin{aligned}\frac{\mathrm{d}\tilde{\omega}}{\mathrm{d}\phi} &= 3\tilde{u}-\frac{3}{4}\left[10+4\eta-(1+10\eta)\tilde{e}^2\right]\tilde{u}^2+\left\{\frac{87}{2}-\left(\frac{877}{35}-\frac{123}{32}\pi^2-22\lambda\right)-3\eta^2\right.\\ &\quad \left.-\left[45-\left(\frac{14867}{560}+\frac{123}{128}\pi^2+\frac{11}{2}\lambda\right)\eta+\frac{93}{2}\eta^2\right]\tilde{e}^2+\frac{3}{8}\eta(12-25\eta)\tilde{e}^4\right\}\tilde{u}^3 \qquad (63)\end{aligned}$$

2.4 New orbit elements and conserved quantities

Even though $\tilde{u}$, $\tilde{e}$ and $\tilde{\omega}$ have proved useful for the integration of the motion, they are not very satisfactory from a physical point of view, since they cannot be defined directly using observational quantities. To remedy this, we would like to define new orbital elements from the characteristics of the orbit. But, as we have seen, the nature of the orbit changes with time because of radiation damping. For example, convenient quantities like the angular velocity at the periastron and at the apastron are not well defined as functions of time: if we define them for the *next* periastron or apastron, we get discontinuous functions. In order to work with smooth parameters, we define $\Omega_a(t)$ (resp. $\Omega_p(t)$) as the angular velocity of the effective body at the next apastron (resp. periastron), *supposing that the radiation reaction has been "turned off" from this moment t*. Similarly, we define $\hat{\omega}$ as the direction of the next periastron with the same condition. It turns out that this $\hat{\omega}$ coincides with the former $\tilde{\omega}$. Then we define:

$$\hat{e} = \frac{\sqrt{\Omega_p}-\sqrt{\Omega_a}}{\sqrt{\Omega_p}+\sqrt{\Omega_a}}, \qquad \hat{u} = \left(\frac{\sqrt{\Omega_p}+\sqrt{\Omega_a}}{2}\right)^{4/3}. \qquad (64)$$

In the Newtonian limit, these definitions naturally reduce themselves to the classical Newtonian eccentricity and mass/semi-latus rectum ratio. We also note that:

$$\hat{u} = \left[\frac{m\Omega_p}{(1+\hat{e})^2}\right]^{2/3} = \left[\frac{m\Omega_a}{(1-\hat{e})^2}\right]^{2/3} \qquad (65)$$

We can easily express Ω_a and Ω_p, and therefore $\hat{u}$ and $\hat{e}$, as functions of $\tilde{e}$ and $\tilde{u}$. We invert these relations and substitute the expressions of $\tilde{e}(\hat{u},\hat{e})$ and $\tilde{u}(\hat{u},\hat{e})$ into the solution of the equations of motion.

The expressions of m/r and $r^2\dot{\phi}$ to 3.5 post-Newtonian order are too long to be reproduced here. However, in order to give an idea of what they look like, we give them to the first order:

$$\begin{aligned}
\frac{m}{r} &= \left[1 + e\cos(\phi-\omega)\right] u \\
&\quad + \left\{1 - \frac{1}{3}\eta + \left(\frac{7}{3} - \frac{7}{4}\eta\right) e^2 + \left[3 - \frac{4}{3}\eta + \left(\frac{1}{3} - \eta\right) e^2\right] e\cos(\phi-\omega) \right. \\
&\quad \left. - \frac{\eta}{4} e^2 \cos(2\phi - 2\omega)\right\} u^2, \qquad (66) \\
r^2\dot{\phi} &= \frac{m}{\sqrt{u}} \left\{1 + \left[(-4+2\eta)\, e\cos(\phi-\omega) - 2 + \frac{2}{3}\eta + \left(-\frac{2}{3} + 2\eta\right) e^2\right] u\right\}, \qquad (67)
\end{aligned}$$

where we have omitted the hats for more readibility. We can check that the leading term corresponds to the Newtonian solution. Note that $u \equiv \hat{u}$, $e \equiv \hat{e}$ and $\omega \equiv \hat{\omega}$ are now *post-Newtonian* orbital elements, and should not be mistaken for the *Newtonian* u, e and ω introduced before. We found that these results are equivalent to those yielded independently through 2PN order using the Wagoner-Will method developed in [11].

Equations (61), (62) and (63) then become:

$$\begin{aligned}
\frac{\mathrm{d}u}{\mathrm{d}\phi} &= \frac{8}{5}\eta\left(8 + 7e^2\right) u^{7/2} - \frac{1}{630}\left[17832 + 22176\eta \right. \\
&\quad \left. - (18976 - 115080\eta)e^2 - (18001 - 27384\eta)e^4\right] u^{9/2}, \qquad (68) \\
\frac{\mathrm{d}e}{\mathrm{d}\phi} &= -\frac{1}{15}\eta e\left(304 + 121e^2\right) u^{5/2} + \eta e\left[\frac{367}{7} + \frac{4336}{45}\eta \right. \\
&\quad \left. - \left(\frac{12499}{315} - \frac{22061}{90}\eta\right) e^2 - \left(\frac{46289}{2520} - \frac{797}{15}\eta\right) e^4\right] \tilde{u}^{7/2}, \qquad (69) \\
\frac{\mathrm{d}\omega}{\mathrm{d}\phi} &= 3u + \left[\frac{9}{2} - 7\eta + \left(\frac{19}{4} - \frac{9}{2}\eta\right)\right] u^2 + \left\{\frac{27}{2} - \left(\frac{3712}{35} - \frac{123}{32}\pi^2 - 22\lambda\right)\eta + 7\eta^2 \right. \\
&\quad \left. + \left[\frac{137}{4} - \left(\frac{45193}{560} - \frac{123}{128}\pi^2 - \frac{11}{2}\lambda\right)\eta + \frac{53}{2}\eta^2\right] e^2 + \left(\frac{5}{2} + \eta + \frac{45}{8}\eta^2\right) e^4\right\} u^3. \qquad (70)
\end{aligned}$$

Now the problem is entirely solved. On the one hand, equations of the type (66) and (67), pushed to 3.5 order, characterize the motion. On the other hand, (68), (69) and (70) give the effect of the radiation reaction on the orbital elements, as well as the periastron advance.

As we claimed before, E and $\mathbf{J}$ are expected to be conserved in a system exempt from radiation reaction. Ignoring the radiation terms, we substitute the expressions of $\mathbf{x}$ and $\mathbf{v}$ into the definitions of the total energy and the total angular momentum (21)-(28), and obtain:

$$
\begin{aligned}
E/\mu \quad = \quad & -\frac{1}{2}(1-e^2)u + \left[\frac{3}{8}+\frac{1}{24}\eta - \left(\frac{5}{12}-\frac{1}{12}\eta\right)e^2 + \left(\frac{1}{24}-\frac{1}{8}\eta\right)e^4\right]u^2 \\
& + \left[\frac{27}{16}-\frac{19}{16}\eta+\frac{1}{48}\eta^2 - \left(\frac{115}{48}+\frac{13}{16}\eta+\frac{7}{48}\eta^2\right)e^2\right. \\
& \left. + \left(\frac{35}{48}+\frac{125}{48}\eta+\frac{1}{16}\eta^2\right)e^4 - \left(\frac{1}{48}+\frac{29}{48}\eta-\frac{1}{16}\eta^2\right)e^6\right]u^3 \\
& + \left\{\frac{675}{128} - \left(\frac{209323}{8064}-\frac{205}{192}\pi^2-\frac{55}{9}\lambda\right)\eta + \frac{155}{192}\eta^2 + \frac{35}{10368}\eta^3\right. \\
& - \left[\frac{167}{32} - \left(\frac{77659}{3360}-\frac{41}{32}\pi^2-\frac{22}{3}\lambda\right)\eta - \frac{2639}{432}\eta^2 + \frac{65}{2592}\eta^3\right]e^2 \\
& - \left[\frac{439}{576} - \left(\frac{305393}{60480}+\frac{41}{192}\pi^2+\frac{11}{9}\lambda\right)\eta + \frac{3727}{864}\eta^2 - \frac{125}{576}\eta^3\right]e^4 \\
& + \left(\frac{1825}{2592}-\frac{1583}{864}\eta-\frac{503}{144}\eta^2-\frac{5}{32}\eta^3\right)e^6 \\
& \left. + \left(\frac{35}{10368}-\frac{143}{384}\eta+\frac{57}{64}\eta^2-\frac{5}{128}\eta^3\right)e^8\right\}u^4, \qquad (71)
\end{aligned}
$$

$$
\begin{aligned}
\mathbf{J} \quad = \quad & \frac{\mu m}{\sqrt{u}}\left\{1 + \left[\frac{3}{2}+\frac{1}{6}\eta - \left(\frac{1}{6}-\frac{1}{2}\eta\right)e^2\right]u\right. \\
& + \left[\frac{27}{8}-\frac{19}{8}\eta+\frac{1}{24}\eta^2 + \left(\frac{23}{12}-\frac{31}{6}\eta-\frac{1}{4}\eta^2\right)e^2 + \left(\frac{1}{24}-\frac{35}{24}\eta-\frac{1}{8}\eta^2\right)e^4\right]u^2 \\
& + \left[\frac{135}{16} - \left(\frac{209393}{5040}-\frac{41}{24}\pi^2-\frac{88}{9}\lambda\right)\eta + \frac{31}{24}\eta^2\right. \\
& \left(\frac{199}{16} - \left(\frac{318313}{5040}-\frac{41}{24}\pi^2-\frac{88}{9}\lambda\right)\eta + \frac{3013}{216}\eta^2 - \frac{5}{144}\eta^3\right)e^2 \\
& \left.\left.\left(\frac{77}{144}-\frac{6497}{432}\eta+\frac{853}{72}\eta^2+\frac{5}{16}\eta^3\right)e^4 - \left(\frac{7}{1296}+\frac{1}{16}\eta+\frac{1}{8}\eta^2-\frac{1}{16}\eta^3\right)e^6\right]u^3\right\}\mathbf{z}. \qquad (72)
\end{aligned}
$$

Again, we can check that the Newtonian limit is correct.

E and $\mathbf{J}$ are perfectly well-defined physical observable quantities. So it can be convenient to express u and e as functions of $\tilde{E} = E/\mu$ and $\tilde{J} = |\mathbf{J}|/m\mu$. Here we give the results to 1PN order, but the calculation can be done up to 3PN order:

$$
u = \frac{1}{J^2}\left[1 + \frac{2}{3J^2}\left(4+2\eta-(1-3\eta)EJ^2\right)\right], \qquad (73)
$$

$$
e = \sqrt{1+2EJ^2}\left[1 - \frac{1}{2}\frac{E}{1+2EJ^2}\left(4+2\eta-(1-3\eta)EJ^2\right)\right]. \qquad (74)
$$

We have thus established a bijection between (E, J) and (e, u), which will prove particularly useful later.

2.5 Harmonic and ADM gauges

We have to be aware that all these results are valid only in a particular gauge. In the last sections, we have chosen a harmonic gauge in which the equations of motion are simple. Let us recall the definition of a harmonic gauge. In a post-Newtonian expansion, we expect the metric to be close to the flat metric $\eta_{\mu\nu}$. So we define the gravitational-field amplitude:

$$h^{\mu\nu} = \sqrt{-g}g^{\mu\nu} - \eta^{\mu\nu}, \tag{75}$$

where g is the determinant of $g_{\mu\nu}$. The harmonic-coordinate condition reads:

$$\partial_\nu h^{\mu\nu} = 0. \tag{76}$$

This condition is very similar to the Lorentz-gauge condition $\partial_\mu A^\mu = 0$ in electro-magnetism.

Einstein's field equations are a system of ten independent second order partial differential equations on the space-time metric $g_{\mu\nu}$:

$$G^{\mu\nu} = 8\pi T^{\mu\nu}, \tag{77}$$

where $G_{\mu\nu} = R_{\mu\nu} - \frac{1}{2}Rg_{\mu\nu}$ is the Einstein tensor. The contracted Bianchi identity gives the equations governing the motion of the matter:

$$\nabla_\nu G^{\mu\nu} = 0 \quad \Longrightarrow \quad \nabla_\nu T^{\mu\nu} = 0 \tag{78}$$

These equations basically correspond to the conservation of momentum and energy in a curved space.

With the harmonic-coordinate condition, Einstein's equations (77) read:

$$\Box h_{\mu\nu} = 16\pi\tau_{\mu\nu}, \tag{79}$$

where $\Box = \eta^{\mu\nu}\partial_\mu\partial_\nu$ is the flat d'Alembertian operator. The source term $\tau_{\mu\nu}$ can be interpreted as an effective stress-energy pseudo-tensor, and depends on both the matter field and the gravitational field as well as its first derivatives. The Bianchi identity is accounted for by the harmonic condition (76).

There actually is an infinity of distinct harmonic gauges, and the equations of motion will generaly depend on the choice of a particular gauge. The 1PN coefficients are standard. The 2PN coefficients have been computed by several groups: Damour and Deruelle [12, 13], Kopeiken and Grishchuck [14],[15], Blanchet *et al.* [16], Itoh *et al.* [17] and Pati and Will [18, 19]. Iyer and Will [20, 21] showed that there is a two-parameter gauge freedom for the 2.5PN coefficients, and a six-parameter freedom for the 3.5PN coefficients. Equations (13), (15), (18) and (20) correspond to an arbitrary choice within these freedoms.

As for the 3PN coefficients, the computation implemented by Blanchet *et al.* [22, 23] produced logarithmic terms, proportional to $\ln(r/r'_1)$ and $\ln(r/r'_2)$, where r'_1 and r'_2 are constants. In order to remove these logarithms and to make the problem tractable, we used the 3PN *contact* coordinate transformation $x_\mu \to x_\mu + \delta x_\mu$, with [23]:

$$\delta x_\mu = -\frac{22}{3}m_1 m_2 \partial_\mu \left[\frac{m_1}{r_2}\ln\left(\frac{r}{r'_1}\right) + \frac{m_2}{r_1}\ln\left(\frac{r}{r'_2}\right)\right], \tag{80}$$

where r_1 (resp. r_2) denotes the coordinate separation between the considered point and the body 1 (resp. body 2). We note that we have $\Box\delta x_\mu = 0$, except at the location of the two bodies. This ensures that the harmonic condition is still respected in the new gauge. The main effect of this coordinate transformation on the equations of motion is to remove the logarithms, as one can see in (14), (19), (24) and (28), where they are absent.

A totally different approach to the n-body problem, implemented through 3PN order by Damour, Jaranowski and Schäfer [24], and which was proved to be equivalent with the harmonic formulation [25], is to compute the Hamiltonian of the system rather than the equations of motion. Unlike other methods, this one does not use a harmonic coordinate system, but some so-called ADM (Arnowitt-Deser-Misner), or "Hamiltonian" coordinate system.

The Hamiltonian has been computed up to 3PN order. We give it here to 1PN order, the entire formula being too long to fit into this page (see [24] for a complete expression):

$$\begin{aligned} H_{\mathrm{ADM}} &= -\frac{m_1 m_2}{2r} + \frac{p_1^2}{2m_1} + \left[-\frac{p_1^4}{8m_1^3} + \frac{m_1^2 m_2}{2r^2} \right. \\ &\left. + \frac{m_1 m_2}{r} \left(\frac{(\mathbf{n}\cdot\mathbf{p_1})(\mathbf{n}\cdot\mathbf{p_2})}{4m_1 m_2} - \frac{3}{2}\frac{p_1^2}{m_1^2} + \frac{7}{4}\frac{\mathbf{p_1}\cdot\mathbf{p_2}}{m_1 m_2} \right) \right] + 1 \leftrightarrow 2. \end{aligned} \tag{81}$$

Again, we change this two-body problem into an effective one-body problem, by using the simple relation $\mathbf{p} = \mathbf{p_1} = -\mathbf{p_2}$, valid in the center-of-mass frame. Thus we get a new expression for $H_{\mathrm{ADM}}(\mathbf{x}, \mathbf{p})$.

From Hamilton's equations:

$$\frac{\mathrm{d}\mathbf{x}}{\mathrm{d}t} = \nabla_{\mathbf{p}} H_{\mathrm{ADM}}, \qquad \frac{\mathrm{d}\mathbf{p}}{\mathrm{d}t} = -\nabla_{\mathbf{x}} H_{\mathrm{ADM}}, \tag{82}$$

we iteratively extract the equations of motion and write them in the same form as equation (10), with different A and B. Substituting the expression of $\mathbf{p}$ as a function of $\mathbf{v}$ and $\mathbf{x}$ into the Hamiltonian, we obtain the total conserved energy E_{ADM}. Similarly, we get $\mathbf{J}_{\mathrm{ADM}}$ by calculating $\mathbf{x}\times\mathbf{p}$. Harmonic and ADM-Hamiltonian coefficients coincide at 1PN order, but they differ at 2PN and 3PN orders. This is true for both the equations of motion and the expressions of the energy and the angular momentum.

We apply the method described in sections 2.2 and 2.3 on the ADM equations of motion, and find similar expressions as (71) and (72) for the energy and the angular momentum (see Appendix, equ. (177), (178)). We observe two common features in the harmonic and the ADM versions of these expressions: (i) the "circular" parts ($e = 0$) of the formulae coincide. In that case the angular velocity $\Omega = \Omega_a = \Omega_p$ is the same as the one observed from infinity for both harmonic and ADM coordinates; (ii) expressions also coincide for $\eta \to 0$, *i.e.* in the test-mass limit. As mentioned before, the differences between the formulae only occur at 2PN and 3PN. It is actually possible to relate the coordinate positions and velocities in the two gauges. In particular, the relation between $\dot\phi_{\mathrm{ADM}}$ and $\dot\phi_{\mathrm{harm}}$, r_{harm}, *etc.* would allow us to find a relation between $(e_{\mathrm{ADM}}, u_{\mathrm{ADM}})$ and $(e_{\mathrm{harm}}, u_{\mathrm{harm}})$, and thus account for the differences in the coefficients of E and $\mathbf{J}$. We found that a transformation of the type:

$$\begin{aligned}\dot{\phi}_{\rm ADM} &= \dot{\phi}\left\{1+\eta\frac{m}{r}\left[\frac{9}{4}\left(v^2-\frac{m}{r}\right)-\left(\frac{16}{3}+\frac{\eta}{2}\right)\left(\frac{m}{r}\right)^2\right.\right.\\ &\left.\left.+\left(\frac{17}{8}-\frac{21}{4}\eta\right)v^4+\left(\frac{239}{24}+\frac{7}{2}\eta\right)\frac{m}{r}v^2+\dot{r}^2 f\left(\dot{r}^2,\frac{m}{r},v^2\right)\right]\right\},\end{aligned} \quad (83)$$

where we have dropped the subscript "harm" under ϕ, r and v in the second member, and where f is a function, was compatible with the differences observed in the expressions of both the energy and the angular momentum. Since $\dot{r}=0$ at the apastron and periastron, f does not need to be determined.

2.6 Equivalence with the quasi-Keplerian parametrization

We now want to check the validity of our formulae by comparing them to previous results. An elegant method for describing the second post-Newtonian relative motion, called the *generalized quasi-Keplerian parametrization*, has been developped by Damour, Shäfer and Wex in ADM coordinates [26, 27, 28]. In that formalism, the polar motion (r,ϕ) is described by the set of equations:

$$n(t-t_0) = w - e_t\sin w + \frac{f_t}{c^4}\sin v + \frac{g_t}{c^4}(v-w) \quad (84)$$

$$r = a(1-e_r\cos w) \quad (85)$$

$$\phi-\phi_0 = \left(1+\frac{k}{c^2}\right) + \frac{f_\phi}{c^4}\sin 2v + \frac{g_\phi}{c^4}\sin 3v \quad (86)$$

$$v = 2\arctan\left[\left(\frac{1+e_\phi}{1-e_\phi}\right)^{1/2}\tan\left(\frac{w}{2}\right)\right], \quad (87)$$

where n, e_t, f_t, g_t, a, e_r, k, f_ϕ, g_ϕ and e_ϕ are functions of E and J. The dependence in c has been kept so that one can see the post-Newtonian order explicitly.

In order to connect this description to ours, we write the expression of Ω_a and Ω_p in terms of the quasi-Keplerian parameters:

$$\Omega_{a/p} = n\frac{1+\frac{k}{c^2}+2\frac{f_\phi}{c^4}\pm 3\frac{g_\phi}{c^4}}{\sqrt{\frac{1\mp e_\phi}{1\pm e_\phi}}\left(1\mp e_t-\frac{g_t}{c^4}\right)+\frac{g_t}{c^4}+\frac{f_t}{c^4}}. \quad (88)$$

Then, using the definitions (64) as well as the definitions for the quasi-Keplerian parameters in terms of E and J (see [28], p. 991), and expanding the results in powers of $1/c$, we find 2PN expressions for $e_{\rm ADM}(E,J)$ and $u_{\rm ADM}(E,J)$. In the end of section 2.4 we have found similar expressions [(73),(74)] in a harmonic coordinate system. Using the same method in the ADM gauge, we can derive from our results the expressions of $e_{\rm ADM}(E,J)$ and $u_{\rm ADM}(E,J)$ through 3PN order (see Appendix, equ. (179)-(186)). We checked that both methods give the same results with 2PN accuracy.

We now want to prove the exact equivalence between our results in the ADM gauge, written in the same form as (66), (67) and (70), and the quasi-Keplerian parametrization.

Our method will consist in finding the parameters n, e_t, *etc.* as functions of $u_{\rm ADM}$ and $e_{\rm ADM}$ (noted u and e for the ease of presentation) through 3PN order and ignoring 2.5PN contributions. Then, replacing $e_{\rm ADM}(E,J)$ and $u_{\rm ADM}(E,J)$ into these expressions, we will check their consistency with the results given in [28] through 2PN order.

We will begin with the more convenient quantities that we can compare, namely the maximum and the minimum coordinate separations r along the orbit. For this we will have to use:

$$r = a\,(1 + e_r \cos w)\,. \tag{89}$$

Then, writing the ADM 3PN version of (66) with $\phi = \omega$ and $\phi = \omega + \pi$, we obtain the equations:

$$\frac{m}{a}\frac{1}{1-e_r} = (1+e)u + PN|_{\phi=\omega}, \qquad \frac{m}{a}\frac{1}{1+e_r} = (1-e)u + PN|_{\phi=\omega+\pi}, \tag{90}$$

where the abreviation "PN" represents the post-Newtonian corrections. From this system of two equations we deduce a and r as functions of u and e:

$$a = -\frac{1}{u(1-e^2)}\left(1 + a_1/c^2 + a_2/c^4 + a_3/c^6\right) \tag{91}$$

$$e_r = e\left(1 + e_{r,1}/c^2 + e_{r,2}/c^4 + e_{r,3}/c^6\right) \tag{92}$$

The exact expressions of a_1, a_2, a_3, $e_{r,1}$, $e_{r,2}$ and $e_{r,3}$ are given in the appendix.

In order to relate the so-called *eccentric anomaly* w to our familiar ϕ, we write the heuristic relations:

$$\phi - \phi_0 = \left(1 + \frac{k}{c^2}\right) + \frac{f_\phi}{c^4}\sin 2v + \frac{g_\phi}{c^4}\sin 3v + \frac{h_\phi}{c^6}\sin 4v + \frac{i_\phi}{c^6}\sin 5v, \tag{93}$$

$$v = 2\arctan\left[\left(\frac{1+e_\phi}{1-e_\phi}\right)^{1/2}\tan\left(\frac{w}{2}\right)\right], \tag{94}$$

and expand the parameters in powers of $1/c$: $k = k_1 + k_2/c^2 + k_3/c^4$, $f_\phi = f_{\phi,2} + f_{\phi,3}/c^2$ and $g_\phi = g_{\phi,2} + g_{\phi,3}/c^2$. As for e_ϕ, we expand its relation to e in the following manner:

$$e = e_\phi\left(1 + e_1/c^2 + e_2/c^4 + e_3/c^6\right). \tag{95}$$

Then, writing

$$\frac{m}{a}\frac{1}{1-e_r\cos w} = \left\{1 + e\cos\left[(\phi-\phi_0)\left(1 - \frac{\mathrm{d}\omega}{\mathrm{d}\phi}\right)\right]\right\}u + PN|_{\omega=\phi\frac{\mathrm{d}\omega}{\mathrm{d}\phi}}, \tag{96}$$

where $\frac{\mathrm{d}\omega}{\mathrm{d}\phi}$ is given by the ADM version of (70) (see Appendix, equ.(187)), and using $\cos w = \frac{1-\tan^2(w/2)}{1+\tan^2(w/2)}$, we find a 3PN expression for $\tan^2\left(\frac{w}{2}\right)$ as a function of ϕ. We substitute the expressions of $\phi(v)$ (93) and $e(e_\phi)$ (95) into this last result, and expand it in powers of 1/c through 3PN order. As expected, the final expression has the form:

$$\tan^2\left(\frac{w}{2}\right) = \frac{1-e_\phi}{1+e_\phi}\tan^2\left(\frac{v}{2}\right) + PN. \tag{97}$$

Of course, we want this result to agree with (94), and thus impose that the post-Newtonian contributions "PN" cancel out. We obtain three different equations (one for each order). 1PN cancelation yields k_1 and e_1; 2PN cancelation yields k_2, e_2, $f_{\phi,2}$ and $g_{\phi,2}$; 3PN cancelation yields k_3, e_3, $f_{\phi,3}$, $g_{\phi,3}$, h_ϕ and i_ϕ. The expression of

$$e_\phi = e\left(1 + e_{\phi,1}/c^2 + e_{\phi,2}/c^4 + e_{\phi,3}/c^6\right) \tag{98}$$

is obtained by the iterative inversion of (95). The complete 3PN expressions of k, f_ϕ, g_ϕ, h_ϕ, i_ϕ and e_ϕ are given in the appendix.

Our last set of parameters involves the evolution of the system with respect to time:

$$n(t - t_0) = w - e_t \sin w + \frac{f_t}{c^4}\sin v + \frac{g_t}{c^4}(v - w) + \frac{h_t}{c^6}\sin(2v) + \frac{i_t}{c^6}\sin(3v). \tag{99}$$

In the formalism developped in section 2.4, the angular velocity $\dot{\phi}$ can be derived from the combination of the ADM 3PN versions of (66) and (67):

$$\dot{\phi} = u^{3/2}[1 + e\cos(\phi - \omega)]^2 + PN. \tag{100}$$

In the quasi-Keplerian parametrization, the same quantity reads:

$$\dot{\phi} = \frac{n\left[1 + \frac{k}{c^2} + \frac{2f_\phi}{c^4}\cos(2v) + \frac{3g_\phi}{c^4}\cos(3v) + \frac{4h_\phi}{c^6}\cos(4v) + \frac{5i_\phi}{c^6}\cos(5v)\right]}{\frac{\sqrt{1-e_\phi^2}}{1+e_\phi\cos v}\left[1 - \frac{g_t}{c^4} - \frac{e_t(\cos v + e_\phi)}{1+e_\phi\cos v}\right] + \frac{f_t}{c^4}\cos v + \frac{g_t}{c^4} + \frac{2h_t}{c^6}\cos(2v) + \frac{3i_t}{c^6}\cos(3v)}. \tag{101}$$

We expand the unkwown variables in powers of $1/c$:

$$\begin{aligned} n &= \left[u(1-e^2)\right]^{3/2}\left(1 + n_1/c^2 + n_2/c^4 + n_3/c^6\right), & (102)\\ e_t &= e\left(1 + e_{t,1}/c^2 + e_{t,2}/c^4 + e_{t,3}/c^6\right), & (103)\\ f_t &= f_{t,2}/c^4 + f_{t,3}/c^6 \qquad g_t = g_{t,2}/c^4 + g_{t,3}/c^6, & (104) \end{aligned}$$

and we equate the two expressions of $\dot{\phi}$ (100) and (101). We collect the terms of common powers of $1/c$ and obtain three independent equations, from which we derive the values of n_1, n_2, ..., i_ϕ. The results are given in the appendix.

For each coefficient, one can check the equivalence between the formulae given in the appendix [(147)-(176)] and the ones given in [28] by using the bijection $(E, J) \leftrightarrow (u, e)$ [(177)-(186)].

3 Tidal interactions of two spherical homogeneous stars

In this section we want to determine the characteristics of a system of binary spherical stars in the Newtonian approximation. We can separate the problem in two distinct parts: (i) the “internal” problem, which consists in solving the equations of the internal structure of each star in a given gravitational field and using a given equation of state; (ii) the “external” problem, or the orbital problem, which governs the motion of the center of mass of each star. In a first stage, we will determine the shape taken by each star submitted to the gravitational field generated by the other star (which is at this level considered to be point-like). In a second stage, we will study the effect of this deformation on the gravitational field thus generated. In the case of solid spheres, the shape will remain spherical. Then, according to the Gauss theorem, the force between the two bodies will be the same as for point-masses, namely Gm_1m_2/r^2. But in the case of bodies made of fluid, the tidal forces slightly distort the stars. Then quadrupole moments appear, which give birh to tidal interaction terms.

We will only consider the case of incompressible stars, for which the analytic treatment is the simplest. Other models exist however: Lai and Shapiro [30] developped a method modelling the stars as compressible ellipsoids; more recently, Taniguchi and Nakamura [31] found almost analytic solutions to equilibrium sequences of binary polytropic stars. Nevertheless, we will assume that the incompressible approximation will suffice for our purpose.

3.1 Free oscillations of an isolated star

When unperturbed, the state of an isolated incompressible star is characterized by the gravitational potential U_0, the pressure P_0 and the density ρ_0, defined by:

$$\rho_0(\tilde{\mathbf{x}},t) = \text{cste}, \quad U_0(\tilde{\mathbf{x}},t) = \frac{2\pi}{3}\rho_0\left(3R^2 - r^2\right) \quad \text{and} \quad P_0(\tilde{\mathbf{x}},t) = \frac{2\pi}{3}\rho_0^2\left(R^2 - r^2\right), \tag{105}$$

where the origin of the spherical coordinates $\tilde{\mathbf{x}} = (\tilde{r},\theta,\phi)$ is taken at the center of the star, and where R is the radius of the star. One then defines the “Eulerian” perturbations:

$$\delta\rho(\tilde{\mathbf{x}},t) = \rho(\tilde{\mathbf{x}},t) - \rho_0, \quad \delta U(\tilde{\mathbf{x}},t) = U(\tilde{\mathbf{x}},t) - U_0(\tilde{\mathbf{x}}), \quad \delta P(\tilde{\mathbf{x}},t) = P(\tilde{\mathbf{x}},t) - P_0(\tilde{\mathbf{x}}), \tag{106}$$

and $\boldsymbol{\xi}(\tilde{\mathbf{x}},t)$, the displacement of fluid element. In this study, we are only interested in incompressible “Kelvin” modes, for which $\nabla\cdot\boldsymbol{\xi} = 0$. For these perturbations, Euler's equation reads:

$$\ddot{\boldsymbol{\xi}} + \nabla\chi = 0, \quad \text{with} \quad \chi = \frac{\delta P}{\rho_0} - \delta U. \tag{107}$$

Since the fluid is incompressible, the only parameter we are concerned with is the radial displacement $\xi_r(R,\theta,\phi,t)$, which characterizes the shape of the star. We express this quantity in terms of spherical harmonics:

$$\xi_r(R,\theta,\phi,t) = \sum_{lm}\epsilon_{lm}(t)Y_{lm}(\theta,\phi). \tag{108}$$

Using the conditions of continuity [33] for δU, $\nabla\delta U$ and δP at the surface of the star, along with $\Delta\delta U = 0$ and $\Delta\delta P = 0$ (obtained from $\nabla \cdot (107)$), we get [33]:

$$\chi = \frac{2M}{R^2}\frac{l-1}{2l+1}\left(\frac{\tilde{r}}{R}\right)^l \epsilon_{lm} Y_{lm}, \tag{109}$$

where we consider only one mode, and where M is the total mass of the star. Euler's equation (107) then reads:

$$\ddot{\boldsymbol{\xi}}_{lm} + \frac{2M(l-1)}{2l+1}\frac{\epsilon_{lm}}{R^{l+2}}\nabla\left(r^l Y_{lm}\right) = 0, \tag{110}$$

from which we deduce [32]:

$$\ddot{\epsilon}_{lm} + \omega_l^2 \epsilon_{lm} = 0, \tag{111}$$

$$\boldsymbol{\xi}_{lm} = \frac{\epsilon_{lm}}{lR^{l-1}}\nabla\left(r^l Y_{lm}\right), \tag{112}$$

$$\text{with} \quad \omega_l^2 = \frac{2Ml(l-1)}{R^3(2l+1)}. \tag{113}$$

The star has got as many independent oscillation modes as there are (l, p) couples. Each one will oscillate with the eigenfrequency ω_l. The $l = 1$ modes will produce "dipole" moments; the $l = 2$ modes "quadrupole" moments; and the $l = 3$ "octupole" moments. In our case the quadrupole modes will be the most important, because they are the first modes to be excited by the tidal potential.

The total kinetic energy of the system is given by:

$$T = \int \rho_0 \left\| \sum_{lm} \dot{\boldsymbol{\xi}}_{lm}(\tilde{\mathbf{x}}, t) \right\|^2 \mathrm{d}^3\tilde{x} = \sum_{lm} \frac{1}{2}\frac{\rho_0 R^3}{l}|\dot{\epsilon}_{lm}|^2, \tag{114}$$

where we have used (112) and the relation:

$$r^2 \int \nabla Y_{lm}^* \cdot \nabla Y_{l'm'}\,\mathrm{d}\Omega = l(l+1)\delta_{ll'}\delta_{mm'}. \tag{115}$$

For more convenience, we introduce the "density perturbation":

$$\tilde{\rho}_{lm}(\tilde{\mathbf{x}}, t) = \rho_0 \epsilon_{lm}\delta(\tilde{r} - R)Y_{lm}, \qquad \rho = \rho_0 + \sum_{lm}\tilde{\rho}_{lm}. \tag{116}$$

The fluid being incompressible, this perturbation is but a calculus trick which will be used to compute integrals over a sphere rather than over the complicated volume described by $\xi_r(R, \theta, \phi)$. We define the internal energy of the system as:

$$U_i = \frac{1}{2}\int \rho\chi\,\mathrm{d}^3\tilde{x} = \sum_{lm}\rho_0 M\frac{l-1}{2l+1}|\epsilon_{lm}|^2. \tag{117}$$

Using (111), the conservation of the total energy $T + U_i$ is straightforward.

3.2 Tidal interactions for irrotational stars

We now consider two identical incompressible stars, denoted by 1 and 2, whose relative position is given by $\mathbf{x} = (r, \Theta, \Phi) = \mathbf{x}_1 - \mathbf{x}_2$, $\mathbf{x}_a$ $(a = 1, 2)$ being the location of the center of mass of the star a in an inertial frame. In the frame associated with the center of mass of 1, using the same notations for 1 as in the previous section, and expressing the tidal contribution from 2 in terms of spherical harmonics, the equations of motion have the following form:

$$\ddot{\boldsymbol{\xi}} + \nabla\chi = \nabla U_T(t), \tag{118}$$

$$\text{with} \quad \nabla U_T = \frac{4\pi M}{r(t)^{l+1}} \sum_{l\geq 2,m} \frac{1}{2l+1} Y^*_{lm}(\Theta(t), \Phi(t)) \nabla \left[\tilde{r}^l Y^*_{lm}(\theta, \phi)\right]. \tag{119}$$

One can show that $\boldsymbol{\xi}$ has the same expression as in (112). Then ϵ_{lm} satisfies [32]:

$$\ddot{\epsilon}_{lm} + \omega_l^2 \epsilon_{lm} = \frac{4\pi M l R^{l-1}}{2l+1} \frac{Y^*_{lm}(\Theta(t), \Phi(t))}{r(t)^{l+1}}. \tag{120}$$

Since $\omega_l^2 \approx M/R^3 \ll M/r^3$, where $\sqrt{M/r^3} \sim \dot{\Phi}/\Phi \sim \dot{r}/r$ corresponds to the characteristic frequency of the orbit, we can specialize to an adiabatic treatement of the problem. Equation (120) has the immediate quasi-static solution:

$$\epsilon_{lm} = \frac{2\pi R}{l-1} \left(\frac{R}{r}\right)^{l+1} Y^*_{lm}(\Theta, \Phi). \tag{121}$$

Note that the corresponding equations for the star 2 can be obtained by making the replacements $\Theta \to \pi - \Theta$ and $\Phi \to \pi + \Phi$. We can now compute the gravitational interaction energy between the two stars. The gravitational potential caused by tidal interactions is given by:

$$V_{12} = \int_1 \int_2 \frac{\rho_1(\tilde{x_1}, t)\rho_2(\tilde{x_2}, t)}{|\tilde{\mathbf{x}}_1 - \tilde{\mathbf{x}}_2 - \mathbf{x}|} \, \mathrm{d}^3x_1 \, \mathrm{d}^3x_2, \tag{122}$$

where ρ_1 and ρ_2 are defined in the same manner as in (116). Using the relations

$$\int Y^*_{lm} Y_{l'm'} \, \mathrm{d}\Omega = \delta_{ll'}\delta_{mm'}, \tag{123}$$

$$\frac{4\pi}{2l+1} \sum_m Y^*_{lm} Y_{lm} = 1, \tag{124}$$

and expressing $(|\tilde{\mathbf{x}}_1 - \tilde{\mathbf{x}}_2 - \mathbf{x}|)^{-1}$ in terms of spherical harmonics, we obtain:

$$V_{12} = 3 \sum_{l\geq 2} \frac{M^2}{l-1} \frac{R^{2l+1}}{r'^{l+1} r^{l+1}} + \frac{M}{r'^2}, \tag{125}$$

where r' represents the *explicit* dependence with respect to the separation between the two stars, r being only involved in the shape of the stars. Restricting our study to the leading contribution $l = 2$, the relative acceleration is:

$$\mathbf{a} = -\frac{2M\mathbf{x}}{r^3} \left[1 + 9\left(\frac{R}{r}\right)^5\right]. \tag{126}$$

From (117) and (121) we deduce, for $l = 2$, the internal energy of both stars:

$$2U_i = \frac{3}{2}\frac{M^2}{r}\left(\frac{R}{r}\right)^5. \tag{127}$$

Defining the orbital kinetic energy as $T_o = (M/4)\mathbf{v}^2$, where $\mathbf{v} = \frac{\mathrm{d}\mathbf{x}}{\mathrm{d}t}$, and the binding energy as $E_b = 2U_i - V_{12}$, we can easily check that the total energy $T_o + E_b$ is conserved at leading order.

3.3 Tidal interactions for rotational stars

The two stars are now rotating with the same angular velocity $\mathbf{\Omega}$, $|\mathbf{\Omega}| \sim \sqrt{M/r^3}$, directed perpendicularly to the plane of the orbit. We redefine (Θ, Φ) as the direction of $\mathbf{x}$ in the corresponding corotating frame. In the corotating frame associated with 1, the equations of motion for the fluid elements of 1 take the form:

$$\ddot{\boldsymbol{\xi}} - \Omega^2 \tilde{\mathbf{x}}_\perp + 2\mathbf{\Omega} \times \dot{\boldsymbol{\xi}} + \dot{\mathbf{\Omega}} \times \tilde{\mathbf{x}} + \nabla\chi = \nabla U_T(t), \tag{128}$$

where $\tilde{\mathbf{x}}_\perp$ is the projection of $\tilde{\mathbf{x}}$ onto the plane of the orbit. The second term of the first member is the inertial centrifuge force; the third term of the first member is the inertial Coriolis force. For the same reasons as in the previous section, we are only interested in quasi-static solutions:

$$\epsilon_{lm} = \frac{2\pi R}{l-1}\left(\frac{R}{r}\right)^{l+1} Y^*_{lm}(\Theta, \Phi) - \frac{1}{3}\sqrt{5\pi}\frac{\Omega^2 R^4}{M r^3}\delta_{l2}\delta_{m0}, \tag{129}$$

Note that we have only kept the divergence-free part of the centrifuge force $\nabla\left(\Omega^2 r^2 \sin\theta^2\right) = \frac{4\sqrt{\pi}}{3}\Omega^2 \nabla\left(r^2\left(Y_{00} - \frac{1}{\sqrt{5}}Y_{20}\right)\right)$. Thus we obtain:

$$V_{12} = 3\frac{M^2 R^5}{r'^3 r^3} + \frac{1}{2}\frac{M\Omega^2 R^5}{r'^3}, \tag{130}$$

$$\mathbf{a} = -\frac{2M\mathbf{x}}{r^3}\left[1 + 9\left(\frac{R}{r}\right)^5 + \frac{3}{2}\frac{\Omega^2 R^5}{r^2 M}\right], \tag{131}$$

$$2U_i = \frac{3}{2}\frac{M^2}{r}\left(\frac{R}{r}\right)^5 + \frac{1}{2}\frac{M\Omega^2 R^5}{r^3} + \frac{1}{6}\Omega^4 R^5. \tag{132}$$

Another energy contribution that we have to take into account is the correction to the rotation kinetic energy due to the distorsion:

$$2T_r = \Omega^2 \sum_{lm} \int \tilde{\rho}_{lm} \tilde{r}^2 \sin^2\theta \, \mathrm{d}r \, \mathrm{d}\Omega = \frac{1}{2}\frac{M\Omega^2 R^5}{r^3} + \frac{1}{3}\Omega^4 R^5. \tag{133}$$

The total energy conservation is not obvious at the first glance. This comes from the fact that the angular velocity Ω is not conserved along the orbit. More precisely, since we have assumed that the displacement $\boldsymbol{\xi}$ is small, we need to make sure that the global displacement does not shift with time. In order to determine $\delta\boldsymbol{\Omega} = \int \mathrm{d}t\,\dot{\boldsymbol{\Omega}}$, we impose: $\int \mathrm{d}^3\tilde{x}\left[\int \mathrm{d}t\left(2\boldsymbol{\Omega}\times\dot{\boldsymbol{\xi}} + \dot{\boldsymbol{\Omega}}\times\tilde{\mathbf{x}}\right)\right] = 0$, and obtain:

$$\delta\boldsymbol{\Omega} = \boldsymbol{\Omega} - \boldsymbol{\Omega}_0 = -\frac{5}{4}\boldsymbol{\Omega}\left(\frac{R}{r}\right)^3, \tag{134}$$

where the angular velocity of reference $\boldsymbol{\Omega}_0$ is taken for an infinite separation. This variation in the angular velocity results in a variation in the rotation kinetic energy:

$$2T'_r = \frac{4M\Omega\delta\Omega R^2}{5} = -\frac{M\Omega^2R^5}{r^3}. \tag{135}$$

Then, with $E_b = 2U_i - V_{12} + 2T_r + 2T'_r$, the total energy $T_o + E_b$ is conserved.

3.4 Solution to the "external" problem

Now that we have the expression of the tidal force for both rotational and irrotational cases, we want to solve the orbital equations of motion to the leading order, taking R/r as a small parameter. For this purpose we use the exact same technique as the one developped in sections 2.2, 2.3 and 2.4. Adding the tidal contributions to the Newtonian force, and using the method of osculating orbit elements, we find the following set of equations:

$$\begin{aligned} p/r \;=\;& 1 + e\cos(\phi-\omega) \\ &+9\left(\frac{R}{p}\right)^5\left[1 + 5e^2 + \frac{15}{8}e^4 + \left(1 + \frac{175}{48}e^2 + \frac{25}{24}e^4\right)e\cos(\phi-\omega)\right. \\ &-\frac{5}{3}\left(1+\frac{1}{2}e^2\right)e^2\cos(2\phi-2\omega) - \frac{5}{16}\left(1+\frac{1}{8}e^2\right)e^3\cos(3\phi-3\omega) \\ &\left.-\frac{1}{24}e^4\cos(4\phi-4\omega) - \frac{1}{384}e^5\cos(5\phi-5\omega)\right] \\ &+3\frac{\Omega^2R^5}{mp^2}\left[1+\frac{1}{2}e^2 + \left(1+\frac{1}{3}e^2\right)e\cos(\phi-\omega) - \frac{1}{6}e^2\cos(2\phi-2\omega)\right] \end{aligned} \tag{136}$$

$$r^2\dot{\phi} = \sqrt{mp}\left[1 - 6\left(\frac{R}{p}\right)^5\left(1+\frac{10}{3}e^2+e^4\right) - 2\frac{\Omega^2R^5}{mp^2}\left(1+\frac{1}{3}e^2\right)\right], \tag{137}$$

$$\begin{aligned} E/\mu \;=\;& -\frac{1}{2}\frac{m}{p}(1-e^2) + \frac{9}{2}\frac{m}{p}\left(\frac{R}{p}\right)^5\left(1+\frac{1}{18}e^2 - \frac{13}{18}e^4 + \frac{1}{6}e^6\right) \\ &+\frac{\Omega^2R^5}{p^3}\left(1-\frac{4}{3}e^2+\frac{1}{3}e^4\right), \end{aligned} \tag{138}$$

$$\frac{\mathrm{d}\omega}{\mathrm{d}\phi} = \frac{45}{2}\left(\frac{R}{p}\right)^5\left(1+\frac{3}{2}e^2+\frac{1}{8}e^4\right) + 3\frac{\Omega^2R^5}{mp^2}. \tag{139}$$

The semi-latus rectum $p = m/u$ and the eccentricity e are defined by (64).

It is important to note that E is the conserved energy defined in the last section (adjusted by an offset such that it goes to 0 for infinite separations), and thus includes corrections to the rotational kinetic energy. In that formulation, Ω is not constant (see equation (134)), but its variations will induce corrections whose order will be higher than required for the expression of this energy. However, the rotational energy, of the type $I\Omega^2$, will have to be computed with the appropriate Ω taken for an infinite separation.

4 Comparison with numerical data

Now that we have PN and tidal formulae at our disposal, we want to compare them with the numerical data given in the litterature. We make the hypothesis that the "helical" condition used in numerical simulations is equivalent to imposing $\dot{r} = 0$. Numerically generated configurations are thus assumed to correspond either to apastrons or to periastrons of slightly eccentric orbits. In those cases, one can use the relations given by (65), and deduce expressions of the energy and the angular momentum as functions of e and Ω only. These expressions will have to be matched with the numerical values of E, J and Ω for each configuration.

Note that the definition of Ω itself is not covariant (gauge independent). However, we know that it becomes covariant for circular orbits. Since we are solely interested in slight eccentricities, we shall assume that gauge-dependences are negligible (actually of order e^2, as one can see from the differences between harmonic (71), (72) and ADM (177), (178) results). We choose to use ADM post-Newtonian formulae, because the numerical simulations use a machinery that bears the same name (even though we do not know exactly whether they use the same coordinate system). We verified that using the harmonic formulae did not sensibly affect our results.

4.1 Irrotational neutron star binary

Formulae given in section 2 are only valid for point-masses. We need to add finite-size corrections in order to fit the numerical data properly. Formally, tidal terms correspond to the 5PN order. But whereas a normal 5PN term is of order $v^{10} \approx (m/r)^5$, tidal terms is of order $(R/r)^5$. In the case of black holes, for which $R \approx m/2$ (m is the total mass), these terms are negligible. But in the case of neutron stars, for which $R \approx 3m$, *i.e.* $(R/r)^5 \approx 250(m/r)^5$, they can become considerable, especially for short separations. We shall only consider Newtonian tidal terms, which means that we shall ignore coupled terms of the kind $(m/r)(R/r)^5$.

The final expression of the energy is obtained by adding up: (i) the Newtonian point-mass term $-(1/2)(1-e^2)u$; (ii) the PN corrections read off from (177); (iii) the rotation-free ($\Omega = 0$) part of the tidal correction read off from (138). u and e are defined using (64), and u is replaced by its expression (65). In order to determine the radius R in our coordinate system, we need to know the covariant, well-defined, circumferencial radius R_c of each star. Then, using the PN relation:

$$R_c = \sqrt{1 + 2\frac{M}{R} + \frac{5}{3}\left(\frac{M}{R}\right)^2}\, R, \tag{140}$$

where M is the irreductible mass of each star, we deduce the value of R. For $M/R_c = 0.14$, we find $M/R = 0.164$. Note that this value coincides within a 10^{-4} error with the radius expressed in the coordinate system used by the numerical code.

As we mentionned before, our hydrodynamic model is based on the assumption that the two stars are made of homogeneous fluid. In the numerical simulation, a polytropic equation of state of the type $P = k\rho^2$ is used. In that configuration, the density distribution is very different from the one we used in our incompressible model. To remedy this problem, we want to correct our tidal term by introducing a prefactor k that would account for the difference between the two density distributions. An appropriate quantity for that purpose, which is involved in the quadrupole formula used in our tidal model, is the moment of inertia of each star. We found $k = I/I_h = 0.6$, where I is the moment of inertia of one isolated star in the numerical simulation, and where $I_h = (2/5)MR^2$ is the moment of inertia of the corresponding homogeneous star.

The final formulae of the *binding energy* E/m then takes the form:

$$E_b = -\frac{\eta}{2}\left(1-e^2\right)\left[\frac{m\Omega_p}{(1-e)^2}\right]^{2/3} + PN + k\frac{9\eta}{2}\left(\frac{R}{m}\right)^5\left(1+\frac{1}{9}e^2-\frac{13}{9}e^4+\frac{1}{3}e^6\right)\left[\frac{m\Omega_p}{(1-e)^2}\right]^4. \tag{141}$$

As for the reduced angular momentum:

$$J/m^2 = \eta\left[\frac{m\Omega_a}{(1-e)^2}\right]^{-1/3} + PN - 6\eta k\left(1+\frac{10}{3}e^2+e^4\right)\left[\frac{m\Omega_a}{(1-e)^2}\right]^{11/3}. \tag{142}$$

Of course, since the two stars are identical, we have $\eta = 1/4$.

The numerical data can be found in [8]. The binding energy is obtained by substracting off the irreductible mass m from the total relativistic energy given in table III of [8], and by scaling the result by m. The value of this irreductible mass is $m = 2 \times 1.5148$ solar masses. We get the reduced angular momentum by scaling the angular momentum given in table III of [8] by m^2.

Results are given in figures 1 and 2. Oddly enough, we observe two very different behaviors depending on the quantity we consider: the numerical values of the energy are best fitted with large eccentricities (~ 0.13) at the apastron, whereas circular orbits fit the numerical values of the angular momentum perfectly.

This suggests that there may be a problem in the respective definitions of the total energy in the numerical and post-Newtionian approaches. Indeed the discrepancy between numerical and analytical results behaves as if there was an “offset” between the two energies. At any rate the question of whether these particular numerical simlulations contain spurious eccentricities remains open.

4.2 Corotational black hole binary

In this case the black holes are spinning with the same angular velocity as the orbital frequency. This means that the two bodies are locked in a configuration where they always present the same side to each other. This particular set of numerical data has already been compared with analytical results in two recent papers [34, 35]. The first one relies on the same method as ours, except that only circular orbits are considered. The second one is based on results from the ADM-hamiltonian approach, and uses Padé resummation methods.

Since we have $R \sim m$ for black holes, tidal terms can be neglected. However, contributions due to the spin of each star will have to be added to the post-Newtonian results. Three distinct sorts of correction will have to be taken into account:

- Rotation contributions. They read $\delta E = (1/2)I\Omega^2$ and $\delta J = I\Omega$ for each star. For black holes, we have $I_a = 4m_a^3$. Thus we obtain: $\delta E/m = 2(1-3\eta)(m\Omega)^2$ and $\delta J/m^2 = 4(1-3\eta)m\Omega$. Those are 2PN contributions.

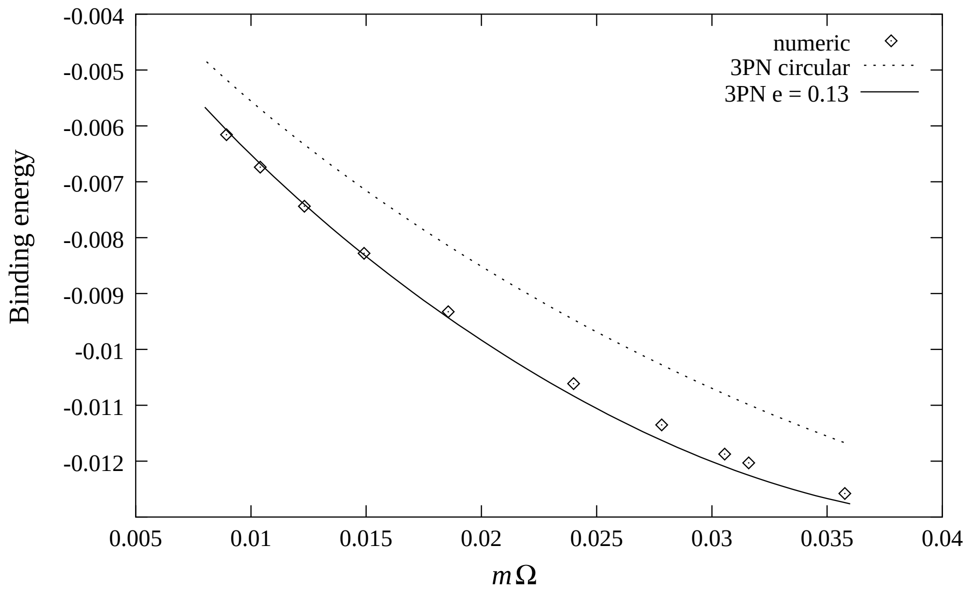

Figure 1: Binding energy *vs.* angular velocity in the case of irrotational neutron stars. Two theoretical curves are plotted: one corresponding to a circular orbit and one corresponding to an eccentric orbit taken at its apastron ($e = 0.13$) for which the numerical values are best fitted.

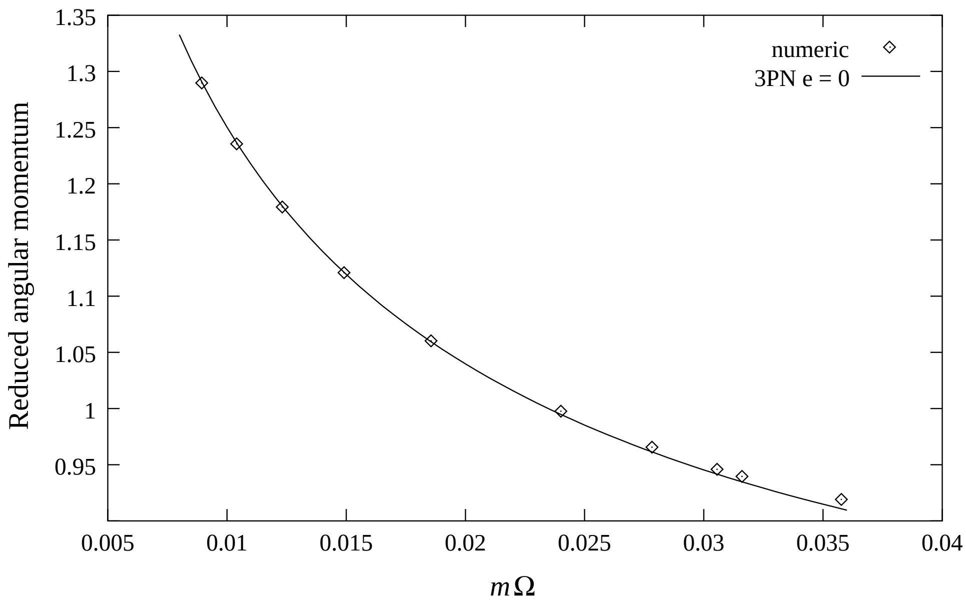

Figure 2: Angular momentum *vs.* angular velocity in the case of irrotational neutron stars. For this quantity the best fit is obtained for a circular orbit.

- Spin-orbit contributions. For that we need the formulae given in [36, 37]. Using $S_a = I\Omega$, we compute the corrections to the energy and the angular momentum in the case of circular orbits. This is justified by the assumption that the eccentricity is small, and by the fact that the spin-orbit contributions are 3PN. We find: $\delta E/m = \eta(-16/3 + 12\eta)(m\Omega)^{8/3}$ and $\delta J/m^2 = 10(-4/3 + 3\eta)(m\Omega)^{2/3}$.
- The replacement of the new total energy (which is also the new attractive mass, modified by the rotation energy) into the Newtonian orbital term. This gives: $\delta E/m = \eta(-2/3 + \eta)(m\Omega)^{8/3}$ and $\delta J/m^2 = \eta(4/3 - 2\eta)(m\Omega)^{5/3}$. Again we only consider the circular part of these 3PN corrections.

We eventually obtain:

$$\delta E/m = 2(1-3\eta)(m\Omega)^2 + \eta\,(-6+13\eta)\,(m\Omega)^{8/3} \quad (143)$$
$$\delta J/m^2 = 4(1-3\eta)m\Omega + 4\eta(-3+7\eta)(m\Omega)^{5/3}. \quad (144)$$

Note that the correction (143) to the energy is consistent with the one found in [34].

Figures 3 and 4 give various analytical fits. If we restrict our study to large separations ($m\Omega < 0.06$), for which PN results are believed to be reliable, we observe discrepancies between analytical and numerical results for both the energy and the angular momentum that cannot be explained by invoking resummation techniques.

Again, the eccentricity required to fit the numerical data depends on the quantity we consider (see fig. 5). This phenomenon resembles the one observed in the case of irrotational neutron stars. In this case however, the qualitative claim that the numerical data sets correspond to apastrons of eccentric orbits is supported by the analysis of both quantities.

4.3 Corotational neutron star binary

This case combines the difficulties of the first two cases. We will have to include: (i) Post-Newtonian terms; (ii) Tidal terms, as well as interaction terms coming from the flattening of each star under the effect of its own rotation [equ. (138)]; (iii) Spin-orbit terms and contributions coming from the replacement of the new attractive mass into the Newtonian part of the binding energy, condensed into the expression: $-(11/10)(R/m)^2(m\Omega)^{8/3}$. The numerical values we are provided with correspond to the energy of the system from which the energy of each star, isolated but spinning with the *same* frequency Ω, has been substracted off. This means for example that the rotation kinetic energy of each star will not have to be included.

One problem remains however: the energy derived in (138) corresponds to the difference between the energy of the binary system and the energy of the same system when the bodies are infinitely separated. But as we mentioned before, the value of Ω, and therefore of the rotation kinetic energy, varies with the separation. Schematically, numerical values correspond to: $E - E_\infty(\Omega)$, whereas our PN-tidal formula corresponds to $E - E_\infty(\Omega_\infty)$. So we have to add the following correction to our analytical formula, according to (134):

$$E_\infty(\Omega_\infty) - E_\infty(\Omega) = \frac{M\Omega^2 R^5}{r^3} \approx \frac{m}{2}\frac{(m\Omega)^4}{1-e}\left(\frac{R}{m}\right)^5 \quad (145)$$

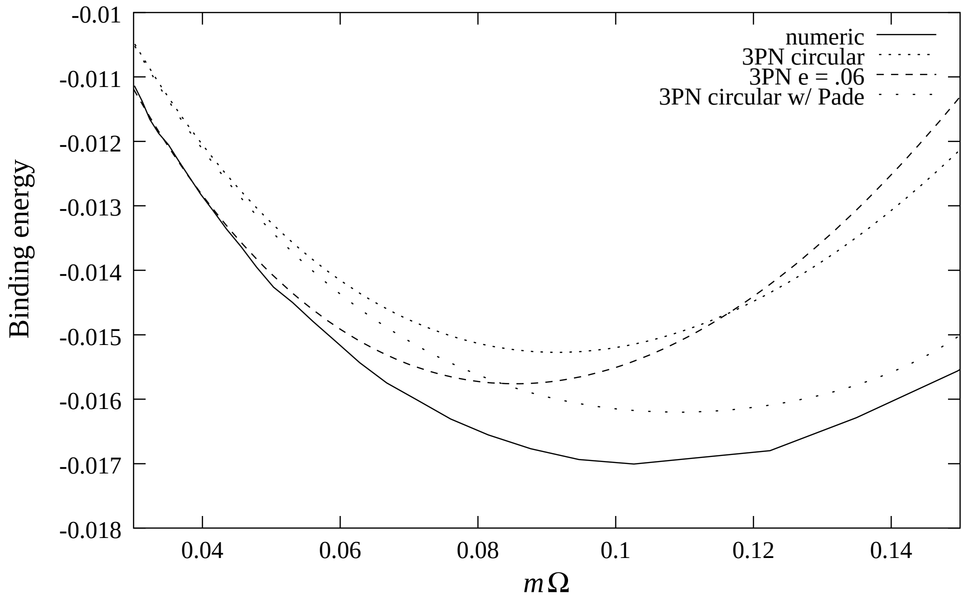

Figure 3: Binding energy *vs.* angular velocity in the case of corotational black holes. Along with the numerical values, we plotted various 3PN analytical curves: simple circular orbits [34]; simple circular orbits with Padé resummation [35]; eccentric orbits corresponding to the best fit of the first ten numerical values.

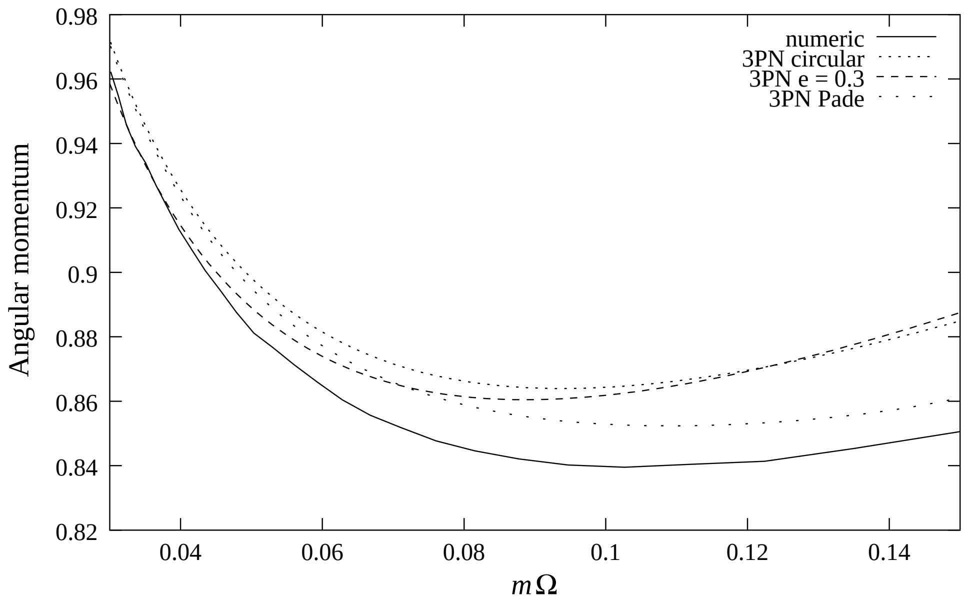

Figure 4: Angular momentum *vs.* angular velocity for corotational black holes. The cases are the same as in figure 3.

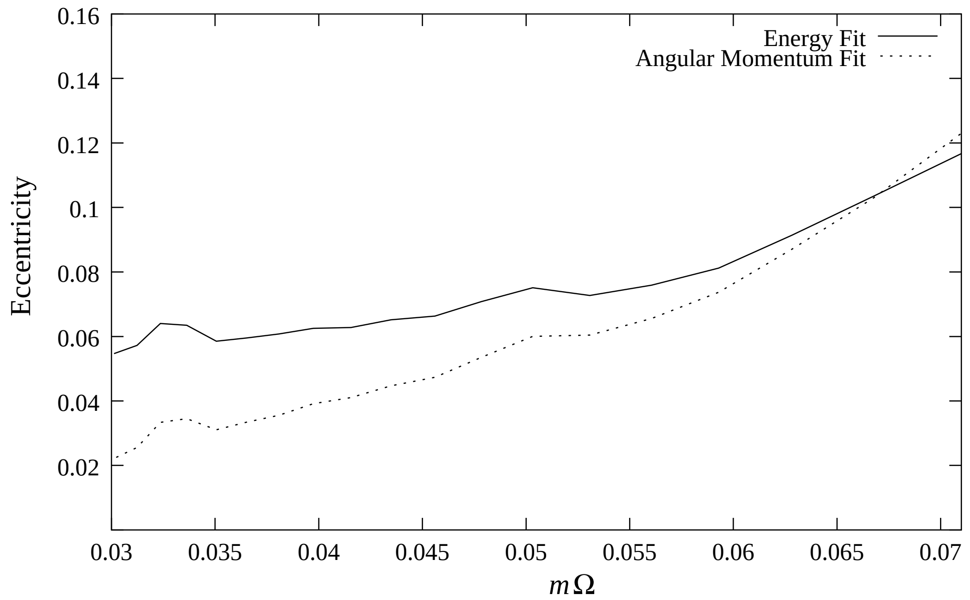

Figure 5: Matching eccentricity *vs.* angular velocity for corotational black holes. For each numerical point we find the eccentricity for which the analytical expression of the energy (resp. angular momentum) coincides with its numerical value.

The remarks about the choice of R and k (see section 4.1) also apply in this case. We found $M/R = 0.1474$ (M is the mass of one star) and $k = 0.62$. The final analytical expression of the energy reads:

$$\begin{aligned} E_b &= -\frac{\eta}{2}\left(1-e^2\right)\left[\frac{m\Omega_a}{(1-e)^2}\right]^{2/3} + PN + k\frac{9\eta}{2}\left(\frac{R}{m}\right)^5\left(1+\frac{1}{9}e^2-\frac{13}{9}e^4\right. \\ &\left.+\frac{1}{3}e^6\right)\left[\frac{m\Omega_a}{(1-e)^2}\right]^4 + k\eta\left(\frac{R}{m}\right)^5\left(1-\frac{4}{3}e^2+\frac{1}{3}e^4\right)\left(\frac{m\Omega_a}{1-e}\right)^4 \\ &-\frac{11}{10}\left(\frac{R}{m}\right)^2(m\Omega_a)^{8/3} + \frac{1}{2}\frac{(m\Omega_a)^4}{1-e}\left(\frac{R}{m}\right)^5 \end{aligned} \quad (146)$$

Energy plots are given in figure 6, and matching eccentricities are given (with error bars) in figure 7. As one can see, the assumption that the numerically generated orbits are circular still holds for these data sets. Besides, the existence of error bars allows us to put boundaries on possible spurious eccentricities.

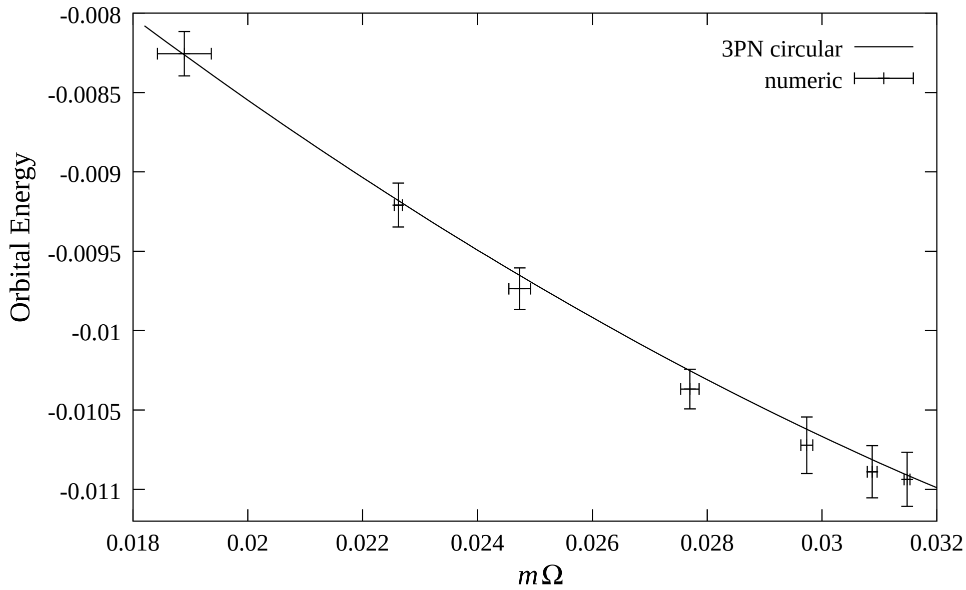

Figure 6: Orbital energy *vs.* angular velocity for corotational neutron stars. The analytical curve corresponding to a circular orbit fits the numerical values correctly.

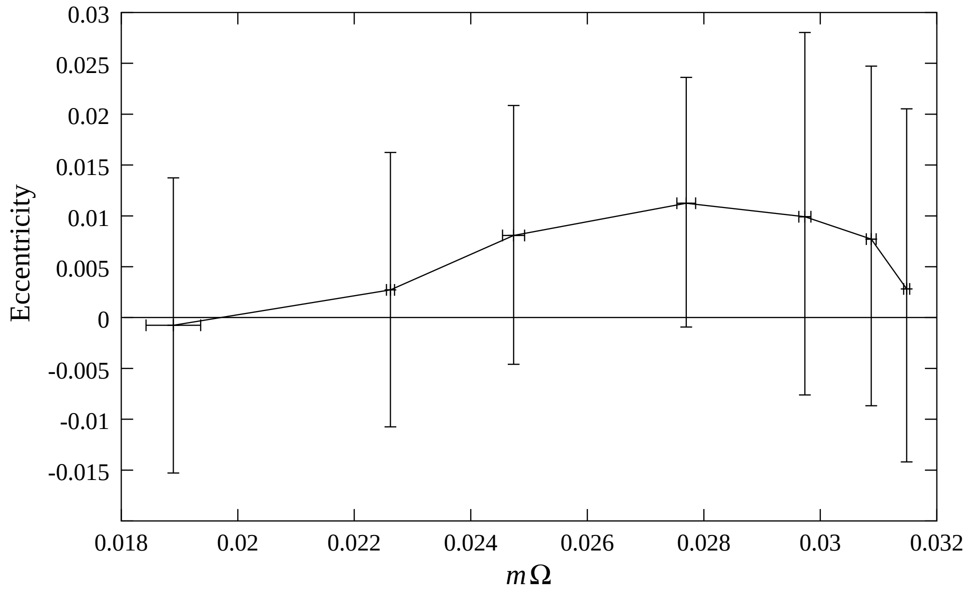

Figure 7: Matching eccentricity *vs.* angular velocity for corotational neutron stars.

5 Conclusion

When I first began this internship, the main objective I was given was to use post-Newtonian methods to account for the observation of spurious eccentricities in *dynamical* numerical simulations made by Mark Miller *et al.* The error leading to this eccentricity could come from three different sources: (i) errors priorly contained in the initial value data set used as initial conditions for the numerical simlulations; (ii) errors coming from the importation of this data set onto a smaller grid for the purpose of the dynamical evolution; (iii) errors coming from the implementation of the numerical evolution itself.

It was clear—and proven—that the value of this spurious eccentricity (of order ~ 0.03) depended on the last two factors (that is, the conditions in which the dynamical evolution was implemented). Yet it was not plain whether the initial data themselves were not fraught with errors. This is what we wanted to check by analysing the energy curves of the initial value data sets. Subsequently we extented our approach to other numerical works [7, 8].

We did not come up with the "nice" definitions of the eccentricity $\hat{e}$ and the semi-latus rectum $\hat{p} = m/\hat{u}$ straightaway. So our first comparisons were based on the only post-Newtonian eccentricity at our disposal back then: $\tilde{e}$. Using this eccentricity, we found very spectacular results for the black hole simulations, in the sense that we could find an almost perfect analytical fit to the energy with a *constant* eccentricity. It turned out later that this was only a coincidence, since $\hat{e} = \tilde{e}(1 + PN\text{corrections})$, for example, is not expected to be constant as $\tilde{e}$ is held constant. In other words, this miraculous fit came from a miraculous choice in the definition of the eccentricity. Nevertheless, the qualitative claim still held as we changed to the new definition.

The conclusions that can be drawn from this study depend on each particular case.

- Corotational neutron stars (figure 7). The presence of error bars allows us to validate the condition of circularity within the range of acknowledged errors. However the question of whether these acknowledged errors can generate spurious eccentricities remains open. But even if they do, we are now able to put boundaries on these eccentricities.

- Corotational black holes (figure 5). We do not dispose of the error bars, which makes the discussion difficult. There no indication whatsoever that the error bars do not overlap the "eccentricity-free" energy and angular momentum curves for large separations (where the PN formulae are reliable). On the other hand, these missing error bars could also account for the difference observed between the matching eccentricities for each quantity.

References

[1] J. H. Taylor and J. M. Weisberg, *Astrophys. J.* **253**, 908 (1982)

[2] L. Blanchet, T. Damour, B. R. Iyer, C. M. Will and A. G. Wiseman, *Phys. Rev. Lett.* **74**, 3515 (1995).

[3] L. Blanchet, T. Damour and B. R. Iyer, *Phys. Rev. D* **51**, 5360 (1995); **54**, 1860 (1996).

[4] C. M. Will and A. G. Wiseman, *Phys. Rev. D* **54**, 4813 (1996).

[5] L. Blanchet, B. R. Iyer and B. Joguet, *Phys. Rev. D* **65**, 061501 (2002), *ibid.* **65**, 064005 (2002).

[6] L. Blanchet, G. Faye, Bala R. Iyer and Benoit Joguet, *Phys. Rev. D* **65**, 061501 (2002).

[7] P. Grandclément, E. Gourgoulhon and S. Bonazzola, *Phys. Rev. D* **65**, 044021 (2002).

[8] E. Gourgoulhon, P. Grandclément, K. Taniguchi, J.-A. Marck and S. Bonazzola, *Phys. Rev. D* **63**, 064029 (2001).

[9] C. W. Lincoln and C. M. Will, *Phys. Rev. D* **42**, 1123 (1990).

[10] L. E. Kidder, C. M. Will and A. G. Wiseman, *Phys. Rev. D* **47**, 3281 (1993).

[11] R. V. Wagoner and C. M. Will, *Astrophys. J.* **210**, 764 (1976); **215**, 984 (1977).

[12] T. Damour and N. Deruelle, *Phys. Lett.* **87A**, 81 (1981).

[13] T. Damour, in *300 Years of Gravitation*, edited by S. W. Hawking and W. Israel (Cambridge University Press, London, 1987), p.128.

[14] S. M. Kopeikin, *Sov. Astron.* **29**, 516 (1985).

[15] L. P. Grishchuk and S. M. Kopeikin, in *Relativity in Celestial Mechanics and Astrometry*, edited by J. Kovalevsky and V. A. Brumberg (Reidel, Dordrecht, 1986), p.19.

[16] L. Blanchet, G. Faye and B. Ponsot, *Phys. Rev. D* **58**, 124002 (1998).

[17] Y. Itoh, T. Futamase and H. Asada, *Phys. Rev. D* **63**, 064038 (2001).

[18] M. E. Pati and C. M. Will, *Phys. Rev. D* **62**, 124015 (2000).

[19] M. E. Pati and C. M. Will, *Phys. Rev. D* **65**, 104008 (2002).

[20] B. R. Iyer and C. M. Will, *Phys. Rev. Lett.* **70**, 113 (1993).

[21] B. R. Iyer and C. M. Will, *Phys. Rev. D* **52**, 6882 (1995).

[22] L. Blanchet and G. Faye, *Phys. Lett.* **271A**, 58 (2000).

[23] L. Blanchet and G. Faye, *Phys. Rev. D* **63**, 062005 (2001).

[24] T. Damour, P. Jaranowski and G. Schäfer, *Phys. Rev. D* **62**, 021501 (2000), *ibid.* **63**, 044021 (2001).

[25] V. C. d'Andrade, L. Blanchet and G. Faye, *Phys. Rev. D* **18**, 753 (2001)

[26] T. Damour and G. Schäfer, *Nuovo Cimento B* **101**, 127 (1988).

[27] G. Schäfer and N. Wex, *Phys Lett.* **174A**, 196 (1993); **177**, 461(E) (1993).

[28] N. Wex, *Class. Quantum Grav.* **12**, 983 (1995).

[29] T. Damour, P. Jaranowski and G. Schäfer, *Phys. Lett.* **513B**, 147 (2001).

[30] D. Lai and S. L. Shapiro, *Astrophys. J.* **443**, 705 (1995).

[31] K. Taniguchi and T. Nakamura, *Phys. Rev. Lett.* **84**, 581 (2000).

[32] C. M. Will, *Astrophys. J.* **274**, 858 (1983).

[33] Chandrasekhar, *Hydrodynamic and Hydromagnetic Stability* (Oxford University Press, 1961).

[34] L. Blanchet, *Phys. Rev. D* **65**, 124009 (2002).

[35] T. Damour, E. Gourgoulhon and P. Grandclément, gr-qc/0204011.

[36] L. E. Kidder, C. M. Will and A. G. Wiseman, *Phys. Rev. D* **47**, R4183 (1993).

[37] L. E. Kidder, *Phys. Rev. D* **52**, 821 (1995).

Appendix: some formulae

Quasi-Keplerian parameters (ADM gauge)

$$n_1 = -\left[3 - \frac{1}{2}(4-\eta)\right] u \tag{147}$$

$$\begin{aligned} n_2 = {} & \left[3 + 4\eta + \left(-\frac{21}{2} + \frac{10}{3}\eta + \frac{1}{6}\eta^2\right) e^2 + \left(\frac{14}{3} - \frac{5}{3}\eta + \frac{3}{8}\eta^2\right) e^4 \right. \\ & \left. + \frac{-\frac{15}{2} + 3\eta + (15 - 6\eta) e^2 + \left(-\frac{15}{2} + 3\eta\right) e^4}{\sqrt{1-e^2}}\right] u^2 \end{aligned} \tag{148}$$

$$\begin{aligned} n_3 = {} & \left\{-21 + \left(\frac{10207}{168} - \frac{55}{3}\lambda - \frac{205}{64}\pi^2\right)\eta + \left(\frac{63}{2} + \left(\frac{1829}{280} + \frac{11}{3}\lambda + \frac{41}{64}\pi^2\right)\eta - \frac{355}{24}\eta^2\right) e^2 \right. \\ & + \left(-34 + \frac{97}{16}\eta - \frac{29}{12}\eta^2 - \frac{5}{12}\eta^3\right) e^4 + \left(\frac{32}{3} - \frac{223}{48}\eta + \frac{19}{12}\eta^2 - \frac{5}{16}\eta^3\right) e^6 \\ & + \left[\frac{15}{2} + \left(\frac{38053}{840} - \frac{11}{3}\lambda - \frac{41}{64}\pi^2\right)\eta - 5\eta^2 + \left(-50 + \left(-\frac{26503}{420} + \frac{22}{3}\lambda + \frac{41}{32}\pi^2\right)\eta + \frac{5}{2}\eta^2\right) e^2 \right. \\ & \left.\left. + \left(\frac{155}{2} - \left(\frac{8147}{840} + \frac{11}{3}\lambda + \frac{41}{64}\pi^2\right)\eta + 10\eta^2\right) e^4 + \left(-35 + \frac{55}{2}\eta - \frac{15}{2}\eta^2\right) e^6\right] / \sqrt{1-e^2}\right\} u^3 \end{aligned} \tag{149}$$

$$e_{t,1} = \left(-2 + \frac{1}{2}\eta\right)\left(1 - e^2\right) u \tag{150}$$

$$\begin{aligned} e_{t,2} = {} & \left\{\frac{21}{4} - \frac{7}{12}\eta + \frac{5}{24}\eta^2 + \left(-\frac{119}{12} + \frac{9}{4}\eta - \frac{7}{12}\eta^2\right) e^2 + \left(\frac{14}{3} - \frac{5}{3}\eta + \frac{3}{8}\eta^2\right) e^4 \right. \\ & \left. + \left[-\frac{15}{2} + 3\eta + \left(\frac{15}{2} - 3\eta\right) e^2\right]\sqrt{1-e^2}\right\} u^2 \end{aligned} \tag{151}$$

$$\begin{aligned} e_{t,3} = {} & \left\{-14 + \left(\frac{3989}{560} - \frac{22}{3}\lambda - \frac{21}{16}\pi^2\right)\eta + \frac{53}{24}\eta^2 + \left[\frac{110}{3} + \left(-\frac{16027}{1680} + \frac{22}{3}\lambda + \frac{21}{16}\pi^2\right)\eta \right.\right. \\ & \left. + \frac{1}{12}\eta^2 - \frac{13}{48}\eta^3\right] e^2 + \left(-\frac{100}{3} + \frac{113}{16}\eta - \frac{31}{8}\eta^2 + \frac{25}{48}\eta^3\right) e^4 + \left(\frac{32}{3} - \frac{223}{48}\eta + \frac{19}{12}\eta^2 - \frac{5}{16}\eta^3\right) e^6 \\ & + \left[\left(\frac{37423}{84} - \frac{11}{3}\lambda - \frac{41}{64}\pi^2\right)\eta - \frac{7}{2}\eta^2 + \left(-35 + \left(-\frac{14323}{840}\frac{11}{3}\lambda + \frac{41}{64}\pi^2\right)\eta - 4\eta^2\right) e^2 \right. \\ & \left.\left. + \left(35 - \frac{55}{2}\eta + \frac{15}{2}\eta^2\right) e^4\right]\sqrt{1-e^2}\right\} \end{aligned} \tag{152}$$

$$f_{t,2} = -\frac{1}{8}\eta e (4+\eta)\left(1-e^2\right)^{3/2} u^2 \tag{153}$$

$$f_{t,3} = \frac{1}{192} e \left[1728 + \left(-3716 + 3\pi^2\right)\eta + 736\eta^2 - 20\eta^3 + \eta\left(-208 + 32\eta + 81\eta^2\right) e^2\right]\left(1-e^2\right)^{3/2} u^3 \tag{154}$$

$$g_{t,2} = \frac{3}{2}(5 - 2\eta)\left(1-e^2\right)^{3/2} u^2 \tag{155}$$

$$\begin{aligned} g_{t,3} = {} & \frac{1}{6720}\left[100800 + \left(-364904 + 24640\lambda + 4305\pi^2\right)\eta + 33600\eta^2 \right. \\ & \left. + \left(134400 - 119280\eta + 40320\eta^2\right) e^2\right]\left(1-e^2\right)^{3/2} u^3 \end{aligned} \tag{156}$$

$$h_t = \frac{1}{32}\eta e^2\left(23 + 12\eta + 6\eta^2\right)\left(1-e^2\right)^{3/2} u^3 \tag{157}$$

$$i_t = \frac{13}{192}\eta^3 e^3 \left(1-e^2\right)^{3/2} u^3 \tag{158}$$

$$a_1 = \left(-1+\frac{1}{3}\eta+\frac{5}{3}e^2\right)u \tag{159}$$

$$a_2 = \left[-\frac{1}{4}+\frac{9}{8}\eta+\frac{1}{9}\eta^2+\frac{1}{72}\left(186-388\eta-24\eta^2\right)e^2+\frac{1}{72}\left(8+75\eta\right)e^4\right]u^2 \tag{160}$$

$$\begin{aligned} a_3 = {} & \left\{-\frac{1}{4}+\left(-\frac{40979}{5040}+\frac{44}{9}\lambda+\frac{167}{192}\pi^2\right)\eta-\frac{3}{2}\eta^2+\frac{2}{81}\eta^3+\left[\frac{23}{3}+\left(-\frac{4019}{140}+\frac{44}{9}\lambda+\frac{41}{48}\pi^2\right)\eta\right.\right. \\ & \left.+\frac{1042}{216}\eta^2-\frac{1}{9}\eta^3\right]e^2+\left[\frac{173}{36}+\left(-\frac{5677}{432}-\frac{1}{64}\pi^2\right)\eta+\frac{16}{3}\eta^2+\frac{1}{3}\eta^3\right]e^4 \\ & \left.+\left(-\frac{2}{81}+\frac{7}{36}\eta-\frac{7}{24}\eta^2\right)e^6\right\}u^3 \end{aligned} \tag{161}$$

$$e_{r,1} = (2-\eta)\left(1-e^2\right)u \tag{162}$$

$$e_{r,2} = \left[\frac{11}{2}-\frac{65}{12}\eta+\frac{1}{3}\eta^2+\left(-\frac{53}{6}+\frac{53}{6}\eta-\frac{1}{3}\eta^2\right)e^2+\left(\frac{10}{3}-\frac{41}{12}\eta\right)e^4\right]u^2 \tag{163}$$

$$\begin{aligned} e_{r,3} = {} & \left\{16+\left(\frac{1991}{48}-\frac{3}{64}\pi^2\right)\eta+\frac{181}{24}\eta^2+\left[-28+\left(\frac{435}{8}+\frac{1}{32}\pi^2\right)\eta-\frac{223}{24}\eta^2-\frac{1}{3}\eta^3\right]e^2\right. \\ & \left.+\left[\frac{52}{3}+\left(-\frac{995}{48}+\frac{1}{48}\pi^2\right)\eta+\frac{79}{24}\eta^2+\frac{1}{3}\eta^3\right]e^4+\left(-\frac{16}{3}+\frac{47}{6}\eta-\frac{37}{24}\eta^2\right)e^6\right\}u^3 \end{aligned} \tag{164}$$

$$k_1 = 3u \tag{165}$$

$$k_2 = \left[\frac{27}{2}-7\eta+\left(\frac{19}{4}-\frac{9}{2}\eta\right)e^2\right]u^2 \tag{166}$$

$$\begin{aligned} k_3 = {} & \left\{\frac{135}{2}+\left(-\frac{5182}{35}+22\lambda+\frac{123}{32}\pi^2\right)\eta+7\eta^2+\left[\frac{251}{4}+\left(-\frac{67873}{560}+\frac{11}{2}\lambda+\frac{123}{128}\pi^2\right)\eta+\frac{53}{2}\eta^2\right]e^2\right. \\ & \left.+\left(\frac{5}{2}-\frac{7}{2}\eta+\frac{45}{8}\eta^2\right)e^4\right\}u^3 \end{aligned} \tag{167}$$

$$f_{\phi,2} = \frac{1}{8}\eta e^2\left(1-3\eta\right)u^2 \tag{168}$$

$$f_{\phi,3} = e^2\left[1+\left(-\frac{12713}{3360}+\frac{11}{12}\lambda+\frac{49}{256}\pi^2\right)\eta-\frac{1}{48}\eta^2+\eta\left(-\frac{23}{192}-\frac{15}{16}\eta+\frac{27}{32}\eta^2\right)e^2\right]u^3 \tag{169}$$

$$g_{\phi,2} = -\frac{3}{32}e^3\eta^2u^2 \tag{170}$$

$$g_{\phi,3} = \eta e^3\left[\frac{55}{192}+\frac{1}{256}\pi^2+\frac{13}{32}\eta+\frac{1}{8}\eta^2+\eta\left(-\frac{1}{16}+\frac{47}{256}\eta\right)e^2\right]u^3 \tag{171}$$

$$h_\phi = \eta e^4\left(\frac{5}{128}+\frac{7}{32}\eta+\frac{5}{64}\eta^2\right)u^3 \tag{172}$$

$$i_\phi = \frac{5}{256}\eta^3e^5u^3 \tag{173}$$

$$e_{\phi,1} = \left(2-\frac{1}{2}\eta\right)\left(1-e^2\right)u \tag{174}$$

$$e_{\phi,2} = \left[\frac{39}{4}-\frac{71}{12}\eta-\frac{1}{3}\eta^2+\left(-\frac{157}{12}+\frac{31}{4}\eta+\frac{35}{96}\eta^2\right)e^2+\left(\frac{10}{3}-\frac{11}{6}\eta-\frac{1}{32}\eta^2\right)e^4\right]u^2 \tag{175}$$

$$\begin{aligned} e_{\phi,3} = {} & \left\{53+\left(-\frac{113467}{840}+\frac{44}{3}\lambda+\frac{167}{64}\pi^2\right)\eta+\frac{93}{8}\eta^2-\frac{1}{6}\eta^3+\left[-\frac{224}{3}+\left(\frac{872981}{6720}-\frac{44}{3}\lambda-\frac{667}{256}\pi^2\right)\eta\right.\right. \\ & \left.-\frac{223}{48}\eta^2+\frac{2}{3}\eta^3\right]e^2+\left[27+\left(\frac{71}{64}-\frac{1}{256}\pi^2\right)\eta-\frac{13}{2}\eta^2-\frac{63}{128}\eta^3\right]e^4 \\ & \left.+\left(-\frac{16}{3}+\frac{65}{16}\eta-\frac{23}{48}\eta^2-\frac{1}{128}\eta^3\right)e^6\right\}u^3 \end{aligned} \tag{176}$$

Expressions of $\tilde{E}$ and $\tilde{J}$ as functions of e and u (ADM gauge)

$$\begin{aligned}
\tilde{E} &= -\frac{1}{2}(1-e^2)u + \left[\frac{3}{8} + \frac{1}{24}\eta - \left(\frac{5}{12} - \frac{1}{12}\eta\right)e^2 + \left(\frac{1}{24} - \frac{1}{8}\eta\right)e^4\right]u^2 + \left[\frac{27}{16} - \frac{19}{16}\eta + \frac{1}{48}\eta^2\right. \\
&\quad - \left(\frac{115}{48} - \frac{5}{16}\eta + \frac{7}{48}\eta^2\right)e^2 + \left(\frac{35}{48} + \frac{53}{48}\eta + \frac{1}{16}\eta^2\right)e^4 - \left.\left(\frac{1}{48} + \frac{11}{48}\eta - \frac{1}{16}\eta^2\right)e^6\right]u^3 \\
&\quad + \left\{\frac{675}{128} - \left(\frac{209323}{8064} - \frac{205}{192}\pi^2 - \frac{55}{9}\lambda\right)\eta + \frac{155}{192}\eta^2 + \frac{35}{10368}\eta^3 - \left[\frac{167}{32} - \left(\frac{266857}{10080} - \frac{41}{32}\pi^2\right.\right.\right. \\
&\quad \left.\left. - \frac{22}{3}\lambda\right)\eta - \frac{775}{216}\eta^2 + \frac{65}{2592}\eta^3\right]e^2 - \left[\frac{439}{576} - \left(\frac{91193}{60480} + \frac{41}{192}\pi^2 + \frac{11}{9}\lambda\right)\eta + \frac{3349}{864}\eta^2 - \frac{125}{576}\eta^3\right]e^4 \\
&\quad \left. + \left(\frac{1825}{2592} - \frac{1679}{864}\eta - \frac{13}{18}\eta^2 - \frac{5}{32}\eta^3\right)e^6 + \left(\frac{35}{10368} - \frac{31}{384}\eta + \frac{13}{64}\eta^2 - \frac{5}{128}\eta^3\right)e^8\right\}u^4 \qquad (177)
\end{aligned}$$

$$\begin{aligned}
\tilde{J} &= \frac{1}{\sqrt{u}} + \left[\frac{3}{2} + \frac{1}{6}\eta - \left(\frac{1}{6} - \frac{1}{2}\eta\right)e^2\right]\sqrt{u} + \left[\frac{27}{8} - \frac{19}{8}\eta + \frac{1}{24}\eta^2 + \left(\frac{23}{12} - \frac{35}{12}\eta - \frac{1}{4}\eta^2\right)e^2 + \left(\frac{1}{24}\right.\right. \\
&\quad \left.\left. - \frac{17}{24}\eta - \frac{1}{8}\eta^2\right)e^4\right]u^{3/2} + \left\{\frac{135}{16} - \left(\frac{209393}{5040} - \frac{41}{24}\pi^2 - \frac{88}{9}\lambda\right)\eta + \frac{31}{24}\eta^2 + \left[\frac{199}{16} - \left(\frac{291083}{5040}\right.\right.\right. \\
&\quad \left.\left. - \frac{41}{24}\pi^2 - \frac{88}{9}\lambda\right)\eta + \frac{2077}{216}\eta^2 - \frac{5}{144}\eta^3\right]e^2\left(\frac{77}{144} - \frac{1337}{432}\eta + \frac{271}{72}\eta^2 + \frac{5}{16}\eta^3\right)e^4 \\
&\quad \left. - \left(\frac{7}{1296} - \frac{7}{48}\eta + \frac{3}{8}\eta^2 - \frac{1}{16}\eta^3\right)e^6\right\}u^{5/2} \qquad (178)
\end{aligned}$$

Expressions of e and u as functions of $\tilde{E}$ and $\tilde{J}$ (ADM gauge)

(we dropped the tildes for the ease of presentation)

$$e = \sqrt{1+EJ^2}\,(1+e_1+e_2+e_3) \qquad (179)$$

$$u = \frac{1}{J^2}\,(1+u_1+u_2+u_3) \qquad (180)$$

$$e_1 = \frac{1}{2}\frac{E}{\sqrt{1+2EJ^2}}\left[4+2\eta+(-1+3\eta)\,EJ^2\right] \qquad (181)$$

$$\begin{aligned}
e_2 &= \frac{E}{J^2(1+2EJ^2)^2}\left[-10+7\eta+\left(-33+\frac{57}{2}\eta+\eta^2\right)EJ^2+\left(-21+37\eta+\frac{7}{2}\eta^2\right)E^2J^4\right. \\
&\quad \left.+\left(-\frac{1}{8}+\frac{55}{4}\eta+\frac{23}{8}\eta^2\right)\right] \qquad (182)
\end{aligned}$$

$$\begin{aligned}
e_3 &= \frac{E}{J^4(1+2EJ^2)^3}\left\{-84+\left(\frac{35471}{210}-\frac{88}{3}\lambda-\frac{41}{8}\pi^2\right)\eta-2\eta^2+\left[-457+\left(\frac{401311}{420}-\frac{484}{3}\lambda\right.\right.\right. \\
&\quad \left.\left.-\frac{451}{16}\pi^2\right)\eta-17\eta^2\right]EJ^2+\left[-811+\left(\frac{76633}{42}-\frac{880}{3}\lambda-\frac{205}{4}\pi^2\right)\eta-\frac{107}{2}\eta^2-\eta^3\right]E^2J^4 \\
&\quad +\left[-\frac{939}{2}+\left(\frac{175729}{140}-176\lambda-\frac{123}{4}\pi^2\right)\eta-\frac{597}{8}\eta^2-\frac{11}{2}\eta^3\right]E^3J^6+\left(-\frac{119}{4}+\frac{1179}{8}\eta-\frac{177}{4}\eta^2\right. \\
&\quad \left.\left.-\frac{79}{8}\eta^3\right)E^4J^8+\left(\frac{1}{16}+\frac{47}{16}\eta-\frac{133}{16}\eta^2-\frac{91}{16}\eta^3\right)E^5J^{10}\right\} \qquad (183)
\end{aligned}$$

$$u_1 = \frac{2}{3}\frac{1}{J^2}\left[4+2\eta+(-1+3\eta)\,EJ^2\right] \tag{184}$$

$$u_2 = \frac{1}{J^4}\left[\frac{176}{9}-\frac{28}{9}\eta+\frac{14}{9}\eta^2+\left(\frac{44}{9}-\frac{86}{9}\eta+\frac{8}{3}\eta^2\right)EJ^2+\left(\frac{5}{9}-7\eta+\eta^2\right)E^2J^4\right] \tag{185}$$

$$\begin{aligned} u_3 = {} & \frac{1}{J^6}\left\{\frac{15232}{81}+\left(-\frac{204986}{945}+\frac{352}{9}\lambda+\frac{41}{6}\pi^2\right)\eta-\frac{236}{27}\eta^2+\frac{140}{81}\eta^3+\left[\frac{2792}{27}+\left(-\frac{228506}{945}+\frac{352}{9}\lambda\right.\right.\right. \\ & \left.\left.+\frac{41}{6}\pi^2\right)\eta-\frac{1042}{27}\eta^2+\frac{28}{9}\eta^3\right]EJ^2+\left(\frac{10}{27}-\frac{475}{27}\eta-\frac{145}{3}\eta^2+\frac{4}{3}\eta^3\right)E^2J^4 \\ & \left.+\left(-\frac{40}{81}+\frac{59}{9}\eta-\frac{44}{3}\eta^2\right)E^3J^6\right\} \end{aligned} \tag{186}$$

Periastron advance (ADM gauge)

$$\begin{aligned} \frac{\mathrm{d}\omega}{\mathrm{d}\phi} = {} & 3u+\left[\frac{9}{2}-7\eta+\left(\frac{19}{4}-\frac{9}{2}\eta\right)e^2\right]u^2+\left\{\frac{27}{2}+\left(-\frac{3712}{35}+22\lambda+\frac{123}{32}\pi^2\right)\eta+7\eta^2\right. \\ & \left.+\left[\frac{137}{4}+\left(-\frac{52753}{560}+\frac{11}{2}\lambda+\frac{123}{128}\pi^2\right)\eta+\frac{53}{2}\eta^2\right]e^2+\left(\frac{5}{2}-\frac{7}{2}\eta+\frac{45}{8}\eta^2\right)e^4\right\}u^3 \end{aligned} \tag{187}$$

Abstract

We make comparisons between fully relativistic numerical computations of quasi-equilibrium configurations of compact binaries (containing either black holes or neutron stars), and post-Newtonian results derived from the perturbative approach to general relativity. To proceed, we develop a method allowing to solve iteratively the post-Newtonian two-body problem using the technique of osculating elements, and we show that our results are consistent with previous works. Then we present a simple hydrodynamic model accounting for tidal interactions between two neutron stars. Post-Newtonian expressions of the energy and the angular momentum — including tidal corrections in the case of neutron stars — are thus derived through third order beyond Newtonian gravity ($O(v/c)^6$) in both rotational and irrotational configurations, and compared to numerically generated values. We showed that the discrepancy sometimes observed for large separations can be accounted for by considering a slightly eccentric orbit taken at its apastron (maximum separation between the two bodies) instead of a circular orbit. This suggests that the errors generated by the approximations made in solving the initial value problem numerically may actually result in the introduction of a spurious eccentricity.

Résumé

Nous comparons des calculs numériques entièrement relativistes de configurations en quasi-équilibre de couples de corps compacts (trous noirs ou étoiles à neutron) avec les résultats post-newtoniens déduits de l'approche perturbative de la relativité générale. Pour ce faire, nous développons une méthode permettant de résoudre le problème post-newtonien des deux corps de manière itérative en utilisant la technique des éléments osculateurs, et nous montrons l'équivalence de nos résultats avec des travaux précédents. Puis nous présentons un modèle hydrodynamique simple rendant compte des interactions de marées subies par deux étoiles à neutron. Nous obtenons ainsi les expressions post-newtoniennes — contenant les termes de marées dans le cas des étoiles à neutron — de l'énergie et du moment cinétique jusqu'au troisième ordre au delà de la limite newtonienne ($O(v/c)^6$) pour des configurations co-rotationelles et irrotationelles, et nous les comparons avec les valeurs obtenues numériquement. Nous avons montré que la différence parfois observée pour les grandes séparations pouvait s'expliquer en considérant, à la place d'une orbite circulaire, une orbite légèrement excentrique prise à son apogée. Cela suggère que les erreurs engendrées par les approximations concédées lors de la résolution numérique du problème de la valeur initiale pourraient bien se manifester par l'introduction d'une excentricité factice.